Thesis for the degree of Doctor of Philosophy
in the Natural Sciences

Structure-based drug design applied to the antibacterial target MraY

On the route to novel antibiotics

Jenny Hering

UNIVERSITY OF GOTHENBURG

Department of Chemistry and Molecular Biology
Gothenburg, 2019

Thesis for the degree of Doctor of Philosophy
in the Natural Sciences

Structure-based drug design applied to the antibacterial target MraY - On the route to novel antibiotics

Jenny Hering

Cover: Inhibition of the antibacterial target MraY by tunicamycin.

ISBN 978-7833-756-9 (Print)
ISBN 978-91-7833-757-6 (PDF)
Available online at http://handle.net/2077/62494

Department of Chemistry and Molecular Biology
Division of Biochemistry and Structural Biology
University of Gothenburg
SE-405 30, Göteborg, Sweden
Printed by BrandFactory AB
Göteborg, Sweden, 2019

Abstract

Antibiotic resistance is one of the biggest threats to human health of our time. We are being warned of a so-called post-antibiotic era, where a simple surgery or bacterial infection could kill human beings. Without the rapid development of novel antibiotics, the continued growth of antibiotic resistance will put our society in a crisis of unprecedented scale.

The bacterial cell wall resembles a protective barrier and is crucial for bacterial survival. Hence, disruption of the cell wall synthesis will lead to cell death. The bacterial membrane protein MraY is involved in the peptidoglycan synthesis, which is a component of the bacterial cell wall, by catalysing the synthesis of lipid I - a peptidoglycan precursor. In this thesis, functional and structural studies of MraY with inhibitors were performed with the future aim of designing novel antibiotics. We solved the crystal structure of MraY from the Gram-positive pathogen *Clostridium bolteae* in complex with the natural product inhibitor tunicamycin at 2.6 Å resolution and provided a biophysical characterisation of the binding mode of tunicamycin. A structural comparison between MraY and its human homolgue GPT identified regions to modify tunicamycin to selectively target MraY. We modified and purified tunicamycins to explore their inhibitory effect and potency towards MraY and identified potent MraY inhibitors with reduced eukaryotic toxicity. Finally, we optimised the purification protocol for MraY for future biophysical and structural studies and developed a novel method using teabags for membrane protein purification.

Acknowledgements

Working on this project was more than challenging and forced me to push my boundaries. The topic is truly urgent, and - if unaddressed - could lead to a crisis of unprecedented scale. It is up to all of us to change the way we use antibiotics in our society. I hope that my work can contribute to the fight against the ongoing growth of antibiotic resistance.

To my supervisors Gisela and Margareta: I am very grateful that I had the opportunity to work with you on this challenging project and I thank you both for your support throughout this thesis. Thanks Gisela, for sharing your knowledge and expertise. Thanks Maggan, for your eye for details and for always supporting me.

Arjan, it was a pleasure working with you. I am so grateful for all discussions, helpful advice and support throughout this thesis. It was an honor being your lab-bench neighbour!

To Per-Olof: You have helped me so much during my thesis with your in-depth knowledge of NMR; thank you for helping me with performing the NMR experiments and for all your advice and your kind-heartedness.

I would like to thank all co-authors and collaborators, it was a pleasure to work with all of you!

To the Structure and Biophysics team at AZ: I thank every single one of you for your support during my PhD. It was a great time and I will miss all of you! Thank you for all lunch breaks, fikas and after-works!

I also thank the entire protein team for creating such a great atmosphere in the lab and for your support!

An meine Familie: Mama, Thorsten und Vera - vielen Dank fuer eure Unterstuetzung in dieser schweren Zeit, ohne euch wäre diese Arbeit niemals möglich gewesen!

Emil, I am so grateful that I made the decision to come to Sweden - meeting you was the best thing that has ever happened to me. You have supported me during my PhD in so many ways that there are no possible words to express how grateful I am. I am glad that the PhD is finally over and I am looking forward to begin our next chapter in life together! Jag älskar dig!

Publications

This thesis consists of the following research papers:

PAPER I: J.K. Hakulinen, **J. Hering**, G. Brändén, H. Chen, A. Snijder, M. Ek, and P. Johansson. "MraY–antibiotic complex reveals details of tunicamycin mode of action" *Nature Chemical Biology* vol. 13, no. 3, pp. 265–267, Mar. 2017.

PAPER II: **J. Hering**, E. Dunevall, M. Ek, and G. Brändén, "Structural basis for selective inhibition of antibacterial target MraY, a membrane-bound enzyme involved in peptidoglycan synthesis" *Drug Discovery Today*, vol. 23, no. 7, pp. 1426–1435, Jul. 2018.

PAPER III: **J. Hering***, E. Dunevall*, A. Snijder, M.A. Jackson, T.M. Hartman, N.P.J. Price, G. Brändén and M. Ek.**These authors contributed equally* "Inhibition of the antibacterial target MraY by modified tunicamycins" *Manuscript*, 2019 (submitted).

PAPER IV: **J. Hering***, J. Winkel Missel*, M. Castaldo, M. Ek, P. Gourdon, and A. Snijder. **These authors contributed equally* "The rapid 'teabag' method for high-end purification of membrane proteins" *Manuscript*, 2019.

Contribution report

PAPER I: I expressed the wild-type and mutant proteins and prepared the membranes for the activity data. I planned, performed, analysed and interpreted the activity measurements and prepared the respective figures.

PAPER II: I took part in the design of the study, performed the literature research, analysed and interpreted the data and performed the structural alignment and superimposition. I played a major role in writing the manuscript and preparing the figures.

PAPER III: I established the purification protocol, prepared the membrane fractions and produced the protein. I planned, performed, analysed and interpreted all experiments and established the assays. I took part in writing the manuscript and preparing the figures.

PAPER IV: I established the teabag protocol for purification of CbMraY, produced the protein and planned, performed, analysed and interpreted all experiments with MraY. I took main responsibility for writing the manuscript.

Abbreviations

Here follows a list and short explanation of the different abbreviations used in this thesis.

CbMraY	*Clostridium bolteae* MraY
CMC	Critical micelle concentration
DDM	n-Dodecyl β-D-maltoside
DM	n-Decyl β-D-maltoside
FRET	Fluorescence resonance energy transfer
GlcNAc	N-Acetylglucosamine
GPT	GlcNAc-1-P transferase
IMAC	Immobilized metal affinity chromatography
IPTG	Isopropyl β-D-1-thiogalactopyranoside
ITC	Isothermal titration calorimetry
MD2	Muraymycin D2
MraY	MurNAc-1-P-transferase
MurNAc	*N*-Acetylmuramic acid
PDB	Protein Data Bank
PNPT	Polyprenyl-phosphate *N*-acetylhexosamine 1-phosphate-transferases
QVM	Quinovosamycin
SEC	Size exclusion chromatography
Tun	Tunicamycin

Contents

Chapter 1

Introduction

1.1 Antibiotic resistance - the curse of modern society

Growing up in our modern society gives the impression of infinite security and stability. Strangely enough, the world as we know it with all its comfort and medical innovation has arisen not a long time ago. The dark times are long forgotten and seem ancient, but are not much older than a century.

The invention of synthetic antibacterial agents and the finding of penicillin at the beginning of the 20th century have dramatically changed human civilisation by saving millions of lives [1]. Infectious diseases were thought to be eradicated soon, thanks to the powerful antibiotic drugs. The inventor of penicillin, Alexander Fleming, was the first to predict the rise of possible resistance due to improper usage of the drugs. The golden era of antibiotics occurred in the middle of the 20th century, when the demand for antibiotics in several sectors increased, hence reducing its price. The first cases of antibiotic resistance were detected shortly after the introduction of novel agents to the market. The boom of antibiotics and the finding of new compounds slowly lessened over the coming decades, and no novel antibiotic agents have been developed since the 1980s [2]. Simultaneously, antibiotic resistance has accelerated dramatically and is now considered a major threat to human health and society [1].

The increase of multidrug-resistant bacteria is a clear warning sign. The focus of antibiotic research now only lies in the modification of already

existing drugs. The most significant contributors responsible for the advent of resistant bacterial strains is the consistent misuse of antibiotics - both clinically as well as in agriculture - and sadly enough, the still insufficient knowledge and education about its correct use [3]. Another driving factor is the use of the same or similar antibacterial agents in agriculture as in clinical use, which can favour the spread of resistance between animal and human populations. The use of antibiotics in cattle feed as a growth promoter is yet another example of the irresponsible use of antibiotics [4].

Antibiotic-resistant bacteria are justly named superbugs as they have become a severe threat to human health by causing life-threatening infections. In Europe alone, every year, an estimated 25.000 people die of infections caused by multiple drug resistance (MDR) bacteria and methicillin-resistant *Staphylococcus aureus* (MRSA) are spreading rapidly worldwide [3]. As a matter of fact, the World Health Organization (WHO) is warning of a post-antibiotic era, resulting in more frequent infections that become impossible to treat leading us to a future that might seem very similar to the ancient times, where small injuries and any simple surgery can end deadly [5].

1.2 Antibiotics

1.2.1 Classification

Antibiotics are a type of antimicrobial agents, which are used effectively to treat bacterial infections. Antibiotics can, in general, be classified based on

- the chemical structure
- the action
- the activity
- and the spectrum

of the antibacterial compound. The chemical structure will give information on the chemical composition of the drug while the action describes

the respective targets of the compound. The activity distinguishes between bactericidal or bacteriostatic compounds. A bactericidal agent can kill the bacteria, whereas a bacteriostatic compound inhibits bacterial growth [6]. In the latter case, the immune system of the patient will have to be able to kill the bacteria. Finally, the spectrum distinguishes between narrow or broad-spectrum compounds: broad-spectrum antibacterial agents are active against a variety of bacterial species and therefore, may be used to treat different infectious diseases, whereas narrow-spectrum antibiotics are active against a specific type of bacteria [7].

1.2.2 Antibacterial agents - mode of action

The mode of action describes how the respective antibacterial compounds take action and how they function. The next paragraph will give an overview of the existing targets (illustrated in Figure 1.1)

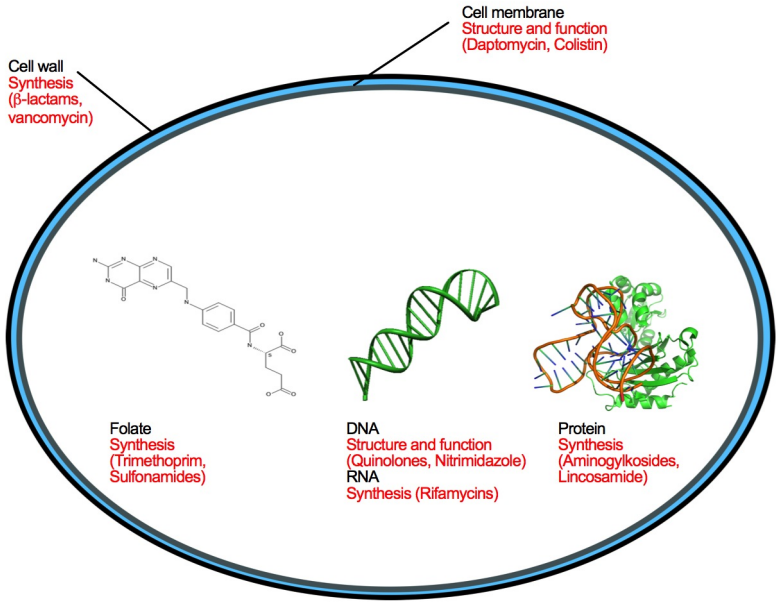

Figure 1.1: Mode of action of antibacterial agents. Simplified schematic of the mode of action of antibiotics illustrating the antibacterial targets of a bacterial cell. The illustration is inspired by [8].

The most common antibiotics act via addressing the bacterial cell wall. Inhibition of the cell wall synthesis will consequently lead to cell disruption and cell death. Other compounds can target the outer cell membrane. These drugs are selective to Gram-negative bacteria and disrupt osmotic integrity. Another way is to act via DNA replication. A possible target would be the topoisomerase, which is a protein that is involved in maintaining the DNA structure. Inhibition of the topoisomerase would lead to cell death as the cells would not be able to replicate. Anti-metabolites-such as folic acid - is another possible target for antibiotics: known inhibitors act by mimicking the substrates of the folic acid synthesis. The last class of target is RNA and protein synthesis. Here the compounds can act either on the nucleotides, on the RNA polymerase or via ribosomal binding [8, 9].

As the number of targets is limited, drug development of antibiotics is narrowed on these few options and focuses on the development of new antibiotics or the modification of existing agents.

1.2.3 Antibiotic resistance - mechanisms and development

Life-threatening infections caused by bacteria that have developed resistance to common antibiotics have become a serious health issue. Those infections are more severe, require more complex treatment and are significantly more expensive. To date, bacteria have become resistant to all classes of antibiotics that are available on the market [3].

The molecular basis for developing resistance to antibiotics is complex and can occur in different ways. Recently, new mechanisms have led to the simultaneous development of resistance to several classes of antibiotics resulting in the dangerous MDR bacterial strains [10]. As antibiotics have the potential to kill bacteria, the latter follow a natural process that stimulates the resistance. Hence, the antibacterial agents induce selective pressure, and the resistance occurs via mutations. In general, mutations leading to resistance can happen spontaneously. However, the most common type of resistance is acquired and occurs via horizontal gene transfer and conjugation of plasmid DNA. In this example, a circular DNA molecule (plasmid) encodes for the antibiotic resistance gene that is transferrable

to other bacterial cells via conjugation. Other types of horizontal gene transfer can occur via transformation - this requires the bacterial cells to be competent, which means they are temporarily more permeable and can take up external DNA - and via transduction - certain types of viruses, so-called macrophages, infect bacteria and with this inject DNA material into the bacterial cells [1].

The acquired development of resistance can also happen endogenously via mutations of chromosomal bacterial DNA. The resistance gene is then transferred vertically to the respective daughter cells.

There are three basic types for the acquired development of resistance:

1. Reduced intracellular accumulation of the drug via reduced or increased influx or efflux of the drug.
2. Enzymatic inactivation of the drug.
3. Modification of the cellular target via
    - mutation
    - chemical modification
    - the protection of the target site or overexpression of a sensitive target for a more resistant one [6].

It is noteworthy to mention that there is also intrinsic, naturally occurring resistance in some bacteria due to structural and functional attributes, which occurs for all members of the bacterial group, e. g. species or genus and can result in the inaccessibility of a drug through the bacterial cell wall [6].

1.3 Bacterial cell wall

The differences in bacterial cell wall structures and the resulting response in the Gram-staining method separated bacteria into two main groups [11]. The cells of Gram-positive and Gram-negative bacteria are composed of

cell wall peptidoglycans that give bacteria their characteristic shape and viability and are exclusive in prokaryotes. The peptidoglycans are composed of a glycan backbone made of *N*-acetylated muramic acid and *N*-acetylated glucosamine. Furthermore, there are highly cross-linked peptide chains in Gram-positive and partially cross-linked peptide chains in Gram-negative bacteria [12].

In Gram-negative bacteria, the cell wall comprises an inner and outer cell membrane that are separated by the periplasm, containing a thin peptidoglycan layer. The presence of an outer membrane is characteristic for Gram-negative bacteria. It contains lipopolysaccharides as a major component of the outer membrane, which is essential for the integrity of the permeability. A capsule polysaccharide (CPS) layer often covers Gram-negative bacteria, and teichoic acids are present in some cases [13]. The peptidoglycan layer in Gram-positive bacteria is substantially thicker compared to Gram-negative bacteria, and they lack an outer membrane. The cell wall of Gram-positive bacteria contains polymers, which are often cross-linked to the peptidoglycan (wall teichoic acids (WTAs)) or can be attached to the cell membrane as lipoteichoic acids (LTAs) [12, 14].

Due to their lack of an outer membrane, Gram-positive bacteria show in general a good permeability for exogenous substances. In contrast, the permeability of the outer membrane of Gram-negative bacteria is low, but pores incorporated to the membrane can regulate the influx.

Mycobacteria and actinobacteria are neither classified as Gram-positive or Gram-negative bacteria due to their unique cell wall composition. The presence of arabinogalactan (AG) - attached to the peptidoglycans and further attached to α-alkyl--hydroxymycolic acids, resulting in a mycolyl-AG-peptidoglycan complex - is characteristic for these bacteria. The complex acts as a permeability barrier leading to natural antibiotic resistance. An outer layer consisting of mycolic acids can relate to the outer membrane of Gram-negative bacteria, even though they share no structural similarity [15].

There are even entirely wall-less bacteria that lack the peptidoglycan layer and are only composed of a cell membrane [16]. As a result of the differences in the cell walls, different antibiotic agents target either Gram-positive or Gram-negative bacteria, Mycobacteria or actinobacteria.

Peptidoglycan synthesis The peptidoglycan, also called murein, is a rigid structure, giving bacteria their cell shape and protection as well as resistance to internal osmotic turgor. The primary chemical composition of peptidoglycan is the same between different genera and consists of parallel strands of linked β-(1-4) disaccharide of *N*-acetylglucosamine (GlcNAc) and *N*-acetylmuramic acid (MurNAc). Peptide strands, connected to MurNAc residues, periodically cross-link the parallel strands - resulting in a 3-dimensional mesh-like structure. The peptidoglycan synthesis (illustrated in Figure 1.2) initiates in the cytoplasm with the synthesis of the nucleotide precursor UDP-MurNAc, which is further converted to UDP-MurNAc-pentapeptide by ATP-dependent amino acid ligases. The disaccharide unit is attached to a carrier lipid C55 polyprenol (C55-P) in the cytoplasmic membrane leading to the formation of lipid I by MraY and further to lipid II by the glycosyltransferase MurG. The lipid-linked disaccharide lipid II is flipped across the cytoplasmic membrane by MurJ and other flippases. At the periplasmic site of the membrane, lipid II is polymerised and new glycan units are inserted into the cell wall, involving glycosyltransferases and transpeptidases (penicillin-binding proteins) [12,14].

1.4 Biological membranes and membrane proteins

Life is highly complex and full of wonders. From the tiniest bacterial species to huge mammalian animals, they all would be incapable of thriving and functioning without biological membranes. These composite structures enable the formation of cells, the basic units of a living organism. A biological membrane is the outer cover layer that separates the cell from its environment - this layer is not rigid but instead fluid and allows movement within the membrane [18]. Due to the composition of a biological membrane, its selective permeability discriminates which substances to exchange with

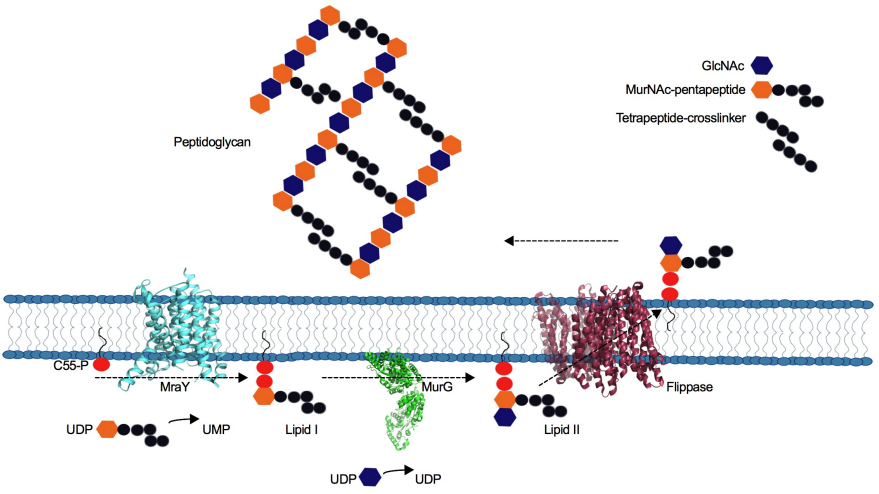

Figure 1.2: Peptidoglycan synthesis. Simplified schematic of the peptidoglycan synthesis illustrating the involved proteins. The illustration is inspired from [17]

.

the environment. The creation of ion gradients across membranes generates energy, and membranes regulate the communication between different cells by receiving or sending information in the form of chemical or electrical signals.

Biological membranes are composed of lipid molecules that form the typical phospholipid bilayer. Next to different types of lipids, membrane proteins and sugars are part of biological membranes. Given the amphipathic composition of lipids, the molecules naturally form a bilayer so that the hydrophilic head groups face towards aqueous solution and the hydrophobic tail groups are pointing inwards facing each other. Membrane lipids will spontaneously form so-called liposomes, which are spheres made of a lipid bilayer, when exposed to aqueous solution. This conformation represents the most favourable state of the lipid molecules thermodynamically [19].

Membrane proteins are vital for the structural integrity of membranes and are the macromolecular machines responsible for cell signalling and the transport of substances through the membranes. Depending on what type of membrane proteins are present in a membrane, different types of signalling molecules can be recognized, and certain chemicals will be permeable through the membrane. Membrane proteins are complex macromolecules with unique biophysical characteristics that determine their structure. Due to their natural occurrence in a lipid bilayer, their biophysical composition differs from soluble proteins, which are exposed to an aqueous solution. Membrane proteins are both in contact with the lipid bilayer as well as the aqueous solution of the respective intracellular or extracellular compartment. However, they are synthesised in the same way as soluble proteins - by ribosomes - and will then be relocated to the designated location of a membrane. This aspect requires challenging or even conflicting demands on the folding and stability of membrane proteins [20].

Knowledge of the structure of membrane proteins can give crucial information about their respective biological function. Many membrane proteins are potential drug targets involved in cell signalling or growth control, which makes them particularly interesting for the pharmaceutical industry [21]. Membrane proteins classify as integral or peripheral membrane proteins. The latter is not embedded into the membrane but instead associated with it, either directly to the phospholipids or indirectly via integral membrane proteins. Integral membrane proteins consist of membrane-spanning domains, which are commonly composed of α-helices or β-barrels. β-barrel membrane proteins usually form pores, with hydrophobic side chains pointing towards the lipid bilayer and the majority of all known β-barrel membrane proteins show hydrophobic amino acids at every second residue in the primary sequence that direct to the interior of the lipid bilayer. This type is near without exception found in the outer membranes of bacterial cells, mitochondria or chloroplasts. In contrast, the α-helical membrane proteins are mostly found in cytoplasmic or subcellular membranes.

In the case of α-helical membrane proteins, there is at least one hydrophobic transmembrane-spanning α-helix, which is composed of approximately 20 amino acids. This transmembrane stretch is around 30 Å long corresponding to the thickness of a phospholipid bilayer. Hydrophobic interactions with the interior of the lipid bilayer stabilise the transmembrane α-helical domains, and hydrophobic side chains of the polypeptide chain shield the polar peptide bonds and form van der Waals interactions with the fatty acid chains. Besides, the carbonyl and imino groups of the peptide bonds form hydrogen-bonds to each other, thus revealing the characteristic helix shape [20].

Important classes of membrane proteins comprise:

- Channels
- Pores
- Transporters
- G-protein-coupled receptors (GPCRs)
- and membrane enzymes.

1.5 MraY and the PNPT superfamily

The PNPT superfamily is a large group of integral membrane enzymes. Their family members are prokaryotic and eukaryotic sugar prenyltransferases, which catalyse the transfer of phospho-*N*-acetylhexosamine from a UDP-*N*-acetylhexosamine sugar nucleotide donor substrate - located in the cytoplasm - to a membrane-bound polyprenyl phosphate acceptor substrate [22]. The prokaryotic family members include the MraY, WecA, TagO, WbcO, WbpL and RgpG enzyme families and are involved in the peptidoglycan synthesis of bacterial cell walls [23]. Despite sharing a common lipid substrate, undecaprenyl-phosphate (C55-P), their distinct UDP-sugar donor substrate distinguishes the family members [24]. The PNPT family contains only one eukaryotic member, UDP-*N*-acetylglucosamine: dolichyl phosphate *N*-acetyl-glucosamine-1-phosphate transferase or GlcNAc-1-P-transferase (GPT) crucial for protein *N*-linked glycosylation and present

in the membrane of the endoplasmic reticulum. GPT uses UDP-GlcNAc as donor substrate and the membrane-bound dolichol phosphate as an acceptor substrate [25].

The PNPT family member MraY (UDP-*N*-acetylmuramyl-pentapeptide: undecaprenyl phosphate *N*-acetylmuramyl-pentapeptide-1-phosphate transferase or MurNAc-1-P-transferase) is a transmembrane enzyme involved in the first membrane-bound step of the peptidoglycan synthesis. Given that MraY is vital for bacterial survival, it is a promising drug target for the development of novel antibiotics, and MraY is only present within the bacterial family members and does not exist in eukaryotes [26].

MraY catalyses the synthesis of the peptidoglycan precursor lipid I (C55-PP-MurNAc-pentapeptide) by using UDP-MurNAc-pentapeptide as the donor substrate and C55-P as the lipid acceptor substrate, resulting in uridine monophosphate (UMP) as a side product, which acts as a weak MraY inhibitor [27,28]. Figure 1.2 illustrates the MraY reaction. A debate was ongoing whether the MraY reaction acts via a one-step or a two-step mechanism [29] and it was concluded from a detailed catalytic study [30] that the reactions occurs via a single displacement mechanism, where both the UDP-sugar substrate and the lipid substrate are bound simultaneously in the active site (**Paper II**).

Studies on different MraY homologues led to expressed and at least partially purified protein [31–33]. Nevertheless, not until 2013, Lee and coworkers [34] solved the first crystal structure of MraY, from the thermophilic *Aquifex aeolicus* (AaMraY), being the first structure of a PNPT superfamily member. Since then, several structures of MraY in complex with inhibitors - including our structure of *Clostridium bolteae* in complex with tunicamycin [35] - have been solved, followed by the recent structures of human GPT. All available structures of the PNPT family members are listed in Table 1.

Structures of the PNPT family members		
Protein/Ligand	**PDB ID**	**Resolution (Å)**
AaMraY/apo [34]	4J72	3.3
AaMraY/MD2 [36]	5CKR	2.96
CbMraY/tunicamycin [35]	5JNQ	2.6
AaMraY/3´-hydroxymureidomcin A [37]	6OZ6	3.7
AaMraY/carbacaprazamycin [37]	6OYH	2.95
AaMraY/capuramycin [37]	6OYZ	3.62
humanGPT/apo [38]	5LEV	3.2
humanGPT/apo [38]	6FM9	3.6
humanGPT/tunicamycin [38]	5O5E	3.4
humanGPT/tunicamycin [39]	6BW5	3.1
humanGPT/tunicamycin [39]	6BW6	2.95
humanGPT/UDP-GlcNAc [38]	6FWZ	3.1

Table 1.1: Crystal structures of the PNPT superfamily members divided into bacterial MraYs and human GPT.

1.6 Tunicamycin

Tunicamycin belongs to a class of natural product inhibitors targeting MraY, including the liposidomycins/caprazamycins, capuramycins, mureidomycins, muraymycins, and tunicamycins. Figure 1.3 illustrates the groups of nucleoside inhibitors with a representative of each group. The uridine-derived nucleoside antibiotic consists of a uridine conjugated to an 11-carbon amino-deoxy dialdose (tunicamine), an *N*-acetylglucosamine sugar (GlcNAc) as well as a fatty acid tail of varying length (13-17 carbons), branching type and saturation. Tunicamycin acquired its name due to its antiviral activity by inhibition of a viral coat, also named "tunica" [12].

Tunicamycin was first identified in *Streptomyces lysosuperificus* in 1973. Due to its ability to block GPT, tunicamycin is a common tool compound to study *N*-linked glycosylation and has been used extensively

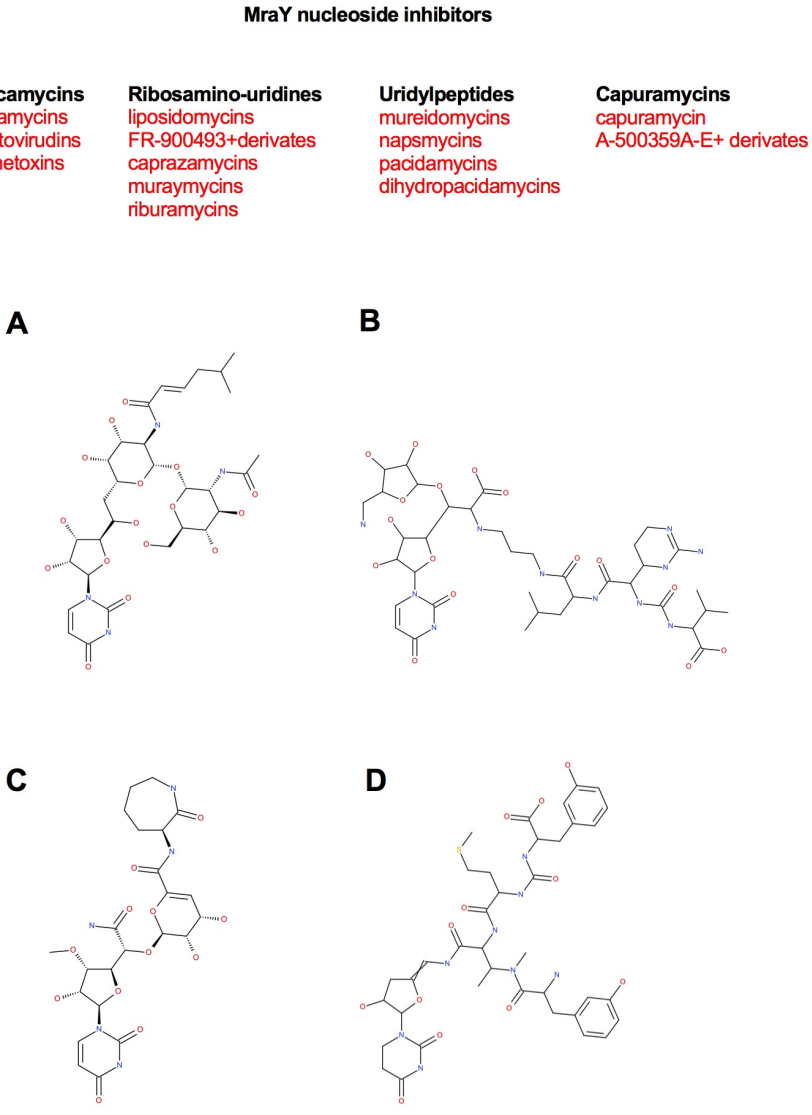

Figure 1.3: The classes of nucleoside inhibitors of MraY. Illustration of the classes of MraY nucleoside inhibitors and their representatives (A) tunicamycin, (B) muraymicin D2, (C) capuramycin and (D) mureidomycin.

since its discovery for studying the role of *N*-glycans in glycoprotein functions [40] [41]. Furthermore, tunicamycin is preferentially inducing apoptosis in cancer cells and is, therefore, a promising compound for use in cancer treatment. Next to its ability to blocking *N*-linked glycosylation, tunicamycin is an effective MraY inhibitor and thereby able to block cell wall synthesis in bacteria. It is instrumental in inhibiting the peptidoglycan synthesis in Gram-positive bacteria but in contrast, shows no activity in Gram-negative bacteria due to its inability to permeate through the outer membrane [42]. Given its effectiveness in inhibiting *N*-linked glycosylation, leading to protein misfolding and cell cycle arrest, tunicamycin is toxic to human cells and therefore not in use as an antibiotic.

Tunicamycin is a potent competitive inhibitor as it resembles the donor nucleotide sugar substrate in the MraY and GPT reactions; it shows IC_{50} values in the range 10 nM to 2000 nM for MraY [42–45] and 9 nM to 200 nM for GPT [39, 46, 47]. Even though tunicamycin shows cytotoxic effects, modified tunicamycins have shown reduced eukaryotic toxicity: reduction of the *trans*-2,3 double bond in the *N*-acyl chain leads to the compound TunR1, and additional reduction of uracil ring - resulting in 5,6-dihydrouracil - leads to compound TunR2 with a significantly reduced toxicity against eukaryotic cell lines [48,49]. Further modification of TunR2 via hydrolytic ring opening reveals TunR3 that shows reduced potency in both bacteria and yeast [48] - which is in agreement with studies on a similar compound in mammalian cells by Hashim and Cushley [50]

Other types of tunicamycin homologues occur besides the classic tunicamycin from *S. lysosuperificus* [41] and *S. chartreusis* [51], including corynetoxins [52]- the *N*-acyl chain is hydrolated -, streptovirudins - the uridine group is replaced by dihydrouracil-, and the quinovosamycins (QVM) - the GlcNAc motif is replaced with QuiNAc [53].

1.7 Structure-based drug design

SStructure-based drug design (SBDD) is the rational design and optimisation of a compound with the potential of becoming a drug candidate

in clinical trials. The history of SBDD begins in the mid-'80s, and the first breakthrough lead to HIV protease inhibitors in the mid-'90s [54, 55]. SBDD is nowadays an integrated part of drug discovery that together with recent advances such as the completion of the Human Genome Project, advances in bioinformatics leading to identification of a vast number of protein targets, and significant progress in molecular and structural biology, has resulted in more than 100.000 protein structures [56, 57].

The process starts with the selection of the target, followed by cloning, gene expression and purification. High throughput screening (HTS) is still the most common way to find starting molecules (hits) where up to 1,000,000 compounds are screened in each project, but other methods can also be used such as fragment screening and virtual library screening. In the next step the molecules are confirmed to bind in an orthogonal assay and structure based drug design is started, that is iterative crystallography support to guide the design of new optimised molecules by visualising the ligand binding in the protein ligand complex. The new compounds are tested for activity and new structures are generated, building an understanding of the structure activity relationship (SAR), improving the affinity and activity. The SBDD involves many design cycles, many structures of the same target but with new compounds are delivered and structural information and guidance how to optimise the molecule is fed into the project. SBDD is of importance also in the lead optimisation phase where the leads have been identified and will be optimised until a candidate drug has been delivered into the development phase where the drugs are developed into medicines. Then the clinical trials are started; Phase 1 (healthy volunteers to test toxicity), Phase 2 (a small population with disease to test efficacy), Phase 3 (final testing at a larger population with disease) and Phase 4 (post approval studies).

1.8 Scope of this thesis

This thesis summarises the work involved with the bacterial membrane protein MraY - including structural and biophysical studies with inhibitors

for the future development of antibacterial agents, and methods to optimise membrane protein purification.
Chapter 2 provides a brief introduction to the methods that I have used throughout this thesis.
Chapter 3 summarises and discusses the results from
Paper I - **Paper IV**.
Chapter 4 is concluding the results and presents future perspectives.

Chapter 2

Methodology

2.1 Expression and purification

The study of membrane proteins is of utmost importance due to their biological and pharmacological significance, even though the experimental procedure is particularly challenging amongst protein biochemists. In order to study the functional and structural characteristics of a membrane protein, the protein has to be extracted from its natural amphiphilic environment and isolated in an active and stable form [58].

The experimental work starts with the overexpression of the protein in a selected host organism; the easiest and cheapest option is the use of bacterial strains as hosts. *Escherichia coli* (*E. coli*) is the most common system for recombinant expression of proteins. In more complicated cases - such as for eukaryotic membrane proteins - the use of eukaryotic cells as expression system may be required due to the lack of specific chaperones and post-translational modifications in prokaryotic systems.

The selected host cells will produce the protein of interest in large amounts. In order to get access to the protein, the cells will be collected by centrifugation and chemically / physically broken (lysed). A centrifugation step will remove the cell debris, and the cell membranes containing the membrane protein of interest are isolated by ultracentrifugation. In the next step, the membrane proteins will be extracted from the membrane by the use of detergents. The resulting membrane protein-detergent micelles are purified by chromatographic methods, and SDS-PAGE (sodium

dodecyl sulfate polyacrylamide gel electrophoresis) and UV-VIS (ultraviolet–visible spectrophotometry) will verify the purity.

Immobilised metal affinity chromatography. Immobilised metal affinity chromatography (IMAC) is a specific type of affinity chromatography, which was first introduced by Porath and coworkers [59] in 1989 and is the most common protein purification method. During IMAC, the proteins are separated due to their specific affinity for certain metal ions, which form chelating complexes with an insoluble matrix, comprised of resin or beads that can be packed to a column [60]. The amino acids histidine, tryptophan and cysteine form complexes with the immobilised metal ions around neutral pH.

In recombinant protein purification, IMAC is commonly used in combination with a poly-histidine fusion, which is tagged to the protein of interest. The poly-histidine tag is a chain of histidine residues located at either the N-terminus or C-terminus of the recombinant protein and has a high affinity for metal ions, which are immobilised to the IMAC matrix. The most commonly used metal ions are Ni^{2+}, Co^{2+}, Cu^{2+} and Zn^{2+} [61]. Other proteins will only bind weakly to the matrix, which are removed during washing steps. Imidazole is a five-membered aromatic molecule containing two nitrogen atoms and is part of the side chain of the amino acid histidine. Therefore, imidazole is competing with the poly-histidine tag for chelating of the metal charged IMAC resin, and thus elutes the recombinant protein. Due to the high affinity of the method, a protein sample of up to 95% purity may be achieved after this single purification step.

Size exclusion chromatography. Size exclusion chromatography (SEC) - or gel filtration chromatography - is usually added as a polishing step after IMAC in order to further purify and optimise the sample quality and homogeneity. During SEC, the proteins and molecules present in the sample will separate according to their size (molecular weight) as they pass through a SEC matrix packed in a column. It is considered as one of the mildest chromatography methods as the molecules do not bind to

the matrix. The SEC matrix or resin consists of porous, spherical particles without adhesive or reactive properties. Once the sample enters the SEC column, molecules that are larger than the pores will elute first. The smaller molecules will penetrate the pores in different ways according to their size, and the ones that can penetrate the pores completely will elute last [62].

Solubilisation of membrane proteins. The probably most critical step during membrane protein purification is the solubilisation of the membrane in order to extract the membrane protein. The aim is to maximally perturb the lipid composition of the membrane and bringing the membrane proteins in an unnatural environment in detergent micelles while maintaining an active and stable conformation - necessary for further experiments [63].

Detergents. Detergents are amphipathic molecules composed of a hydrophilic head group, which is polar or charged, and a hydrophobic carbon tail. Detergents are classified based on their chemical composition as ionic, zwitterionic or non-ionic detergents. Due to their amphipathic structure, the polar head groups form hydrogen bonds with water in aqueous solution, and the hydrophobic tails will aggregate and form hydrophobic interactions. As a result of their unique properties, detergents find applications in the solubilisation of membrane proteins, cell lysis and protein crystallization [64].

In aqueous solution, detergents are present as monomers at low concentrations. Detergent monomers will spontaneously start forming noncovalent micelles above a specific concentration - the critical micelle concentration (CMC). The CMC varies for different detergents and is depending on different factors such as pH, ionic strength and temperature [64]. At concentrations above the CMC, the detergent micelles can form complexes with membrane proteins; thus, the CMC is an essential parameter in membrane protein biochemistry. Detergent micelles represent an amphipathic environment that is similar to phospholipid bilayers, which makes the use of detergents as solubilizing agents so crucial in functional and structural studies of membrane proteins.

At low concentrations, the detergent monomers perturb the phospholipid membrane by partitioning into the bilayer without solubilising the membrane proteins. At concentrations equal to or above the CMC, the membrane bilayer will rupture as it gets saturated with detergent molecules - resulting in lipid-protein-detergent mixed micelles. This event typically occurs at a detergent/protein ratio of 1/2 (w/w) [65]. A further increase in detergent concentration will cause delipidation of the mixed micelles leading to detergent-protein mixed micelles and detergent-lipid mixed micelles. Figure 2.1 sketches the principle of the solubilisation process.

2.1.1 Expression of CbMraY

In this work, *Clostridium bolteae* MraY was recombinantly overexpressed in *E. coli* cells. A detailed description of the method is found in **Paper III**. The CbMraY construct included an N-terminal PelB signal sequence, a TEV cleavable N-terminal split GFP sequence and a C-terminal His10 tag in the pET26b+ plasmid [32, 35]. CbMraY protein was overexpressed in *E. coli* BL21(DE3)Gold cells in Super Broth medium as 500-ml cultures containing kanamycin and D-(+)-Glucose in flasks. Cells were grown to OD600 = 0.7–0.9 at 37 °C and 210 r.p.m (rounds per minute). Protein expression was induced with IPTG at 18°C for 17–18 hours. Harvested cells were resuspended in HEPES (4-(2-hydroxyethyl)-1-piperazineethanesulfonic acid) buffer and either flash-frozen in liquid nitrogen and stored at -80°C or subsequently used for purification.

2.1.2 Preparation of membranes containing overexpressed CbMraY for inhibition measurements.

Membranes containing overexpressed CbMraY wild-type or mutant protein were prepared for the use in inhibition measurements described in section 3. CbMraY proteins were overproduced in *E. coli* BL21(DE3)Gold cells in SB medium as 100-ml cultures and further steps were performed as stated above in section 2.1.1. Freshly harvested or frozen cells were taken in lysis buffer, and cells were lysed in a constant system cell disrupter. The cell debris was removed by centrifugation and membranes were isolated by ultracentrifugation at 138,000 $\times$ g and resuspended in

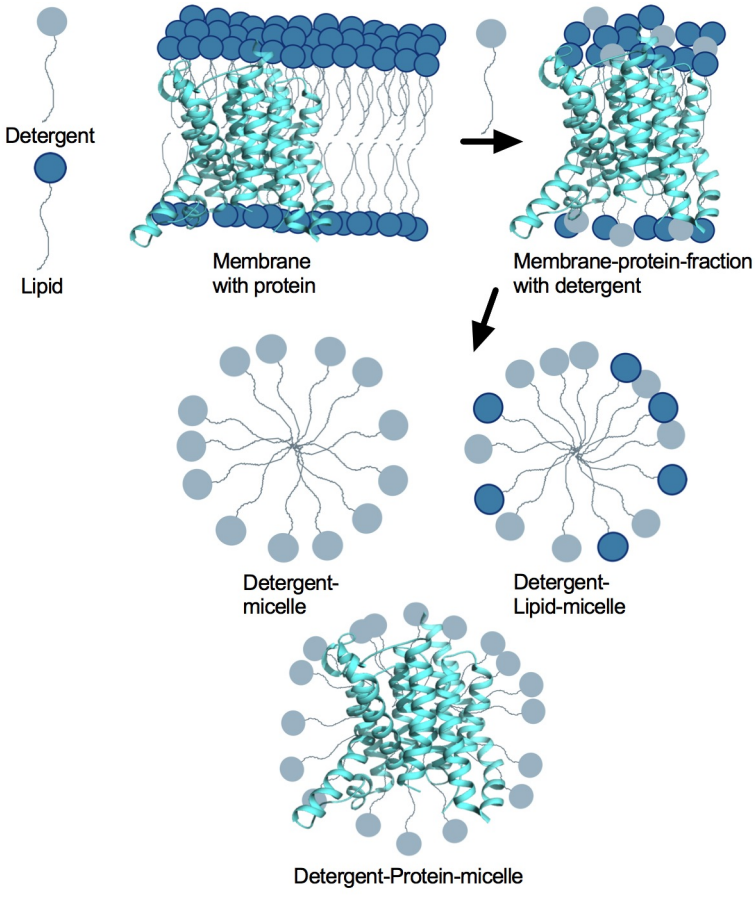

Figure 2.1: The process of solubilisation Simplified scheme of the solubilisation of membrane proteins.

membrane buffer. Equal expression levels of MraY proteins was verified by FSEC (Fluorescence-Detection Size-Exclusion Chromatography). Total membrane protein concentration was determined via Bradford assay (BioRad kit) using a BSA (Bovine Serum Albumin) standard curve.

2.1.3 Purification of CbMraY

All steps were carried out at 4°C. Cells were lysed in a constant system cell disruptor, and protein was extracted from the crude lysate by addition of dodecyl-maltoside (DDM). Insoluble fractions were removed by centrifugation, and the supernatant was incubated with cobalt Talon resin in batch mode overnight and washed with IMAC buffer the following morning. Following IMAC, the detergent was exchanged to decylmaltoside (DM), and protein was eluted in elution buffer containing imidazole. The protein was subsequently concentrated using spin concentrators with 50 kDa cutoff, and size-exclusion chromatography was carried out using a Superdex 200 10/30 column (GE Healthcare) in combination with Äkta system. The protein was stored at 4°C for subsequent experiments or flash-frozen in liquid nitrogen and stored at -80°C.

2.2 Functional studies of CbMraY and ligand interactions

The following section will give a brief overview about the different methods that were used to study the functional characteristics of CbMraY and its interactions with different inhibitors. The methods are described in detail in **Paper I** and **Paper III**.

2.2.1 Enzymatic activity assay

The assay used to measure the enzymatic activity of CbMraY is based on Fluorescence resonance energy transfer (FRET). FRET is a physical process, which involves non-radiative energy transfer from an excited donor fluorophore molecule to an acceptor fluorophore due to intermolecular long-range dipole-dipole coupling [66]. FRET is a highly sensitive, distance-dependent method to investigate molecular proximities in Å-range (10-100 Å). The so-called Förster radius gives the distance at which half of the excitation energy is transferred from the donor to the acceptor fluorophore molecule and typically lies between 3-6 nm [67]. FRET is most efficient if donor and acceptor are oriented within the Förster radius [68, 69].

FRET-based assay to detect MraY enzyme activity The FRET-based assay used to measure MraY enzymatic activity was initially developed by Shapiro and coworkers [44] in a high-throughput set up to screen for MraY inhibitors. The original protocol was designed for measuring MraY activity in membranes. In this work, the protocol was adopted - suitable for small-scale use.

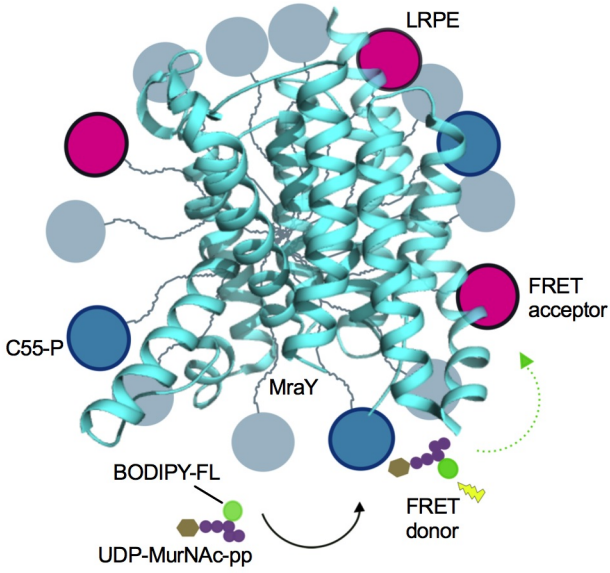

Figure 2.2: Illustration of the FRET-based activity assay. Detergent micelles (grey head groups) contain MraY protein (cyan), undecaprenyl phosphate (C55-P, blue head-groups) and the FRET acceptor LRPE (pink). UDP-MurNAc-pentapeptide is labelled with the FRET donor (BODIPY-FL) and comes in close proximity to the FRET acceptor upon MraY reaction. The illustration is inspired from [17].

In the FRET assay, the donor fluorophore BODIPY-FL with an emission wavelength of 520 nm is attached to the soluble substrate of MraY, UDP-MurNAc-pentapeptide. 1,2-dipalmitoyl-sn-glycero-3-phos-phoethano-lamine-N-(lissamine rhodamine B sulfonyl (LRPE)) acts as acceptor fluorophore with an emission wavelength of 590 nm, which is incorporated in the

lipid-detergent-protein mixed micelles or detergent-protein mixed micelles. During the MraY translocase reaction, UDP-MurNAc-pentapeptide will be attached to C55-P, therefore bringing donor and acceptor fluorophore in proximity sufficient for FRET as illustrated in Figure 2.2. Excitation at 480 nm will initiate FRET, hence reducing the donor fluorescence at 520 nm and increasing the acceptor fluorescence at 590 nm. MraY enzymatic activity is visualised as progress curves by plotting the ratio of F590 nm/F520 nm against the reaction time [44].

In **Paper I**, initial rates were calculated from the change in the 520nm fluorescence signal (ΔF520), which follows the uptake of UDP-MurNAc-pentapeptide for the first two minutes of the reactions using a linear fit. Therefore, the assay was performed in the presence (5mM) and absence (0mM) of UMP, which acts as MraY inhibitor, in order to subtract the baseline. The resulting process curves reflect the MraY enzymatic activity.

2.2.2 Inhibition measurements

The FRET-based activity assay was used in order to investigate the potential inhibition of CbMraY by different compounds. The assay was performed in black well plates in a PheraStar plate reader. *E. coli* membranes containing overexpressed CbMraY were pre-incubated with different concentrations of compounds, C55-P and LRPE in assay buffer before initiating the reaction with UDP-MurNAc-pentapeptide. The compounds were diluted in assay buffer from stock solutions in DMSO. Fluorescence was excited at 485 nm and detected simultaneously at 520nm and 590nm, every minute for 35 minutes. Control experiment to verify MraY activity were performed without compounds and 2% DMSO representing the highest DMSO concentration that was used in the assay. Average progress curves with membranes in the absence of overexpressed CbMraY were subtracted from the average progress curves with membranes containining overexpressed CbMraY to obtain Δ(F590/F520). The first measuring point of the reaction (starting point at 0 minutes) was subtracted from the last (endpoint at 35 minutes) to calculate the response. IC_{50} values were then calculated using a nonlinear regression curve fit with a variable slope (four parameters) in GraphPad Prism version 8.0.0.

2.2.3 Isothermal Titration Calorimetry

Isothermal Titration Calorimetry (ITC) is the measurement of binding affinity and thermodynamic parameters of biomolecular interactions. The method is based on the direct measurement of heat that is either released or absorbed during a binding event under constant temperature. It is a compelling label-free technique that does not require immobilization of the binding partners and thus measures the binding event in solution [70]. During an ITC experiment, one will determine the binding constant K_D, the reaction stoichiometry (n), enthalpy (ΔH) and entropy (ΔS). Careful examination and interpretation of the determined thermodynamic parameters can give a deep insight into molecular mechanisms behind the binding event such as conformational changes [71].

During an ITC experiment, a ligand is gradually titrated from a syringe into a sample cell containing a potential binding partner. In the event of binding, the absorption or release of heat is detected by a sensitive calorimeter. A reference cell containing water is required in order to detect the heat change in case of binding. The sample cell is then readjusted to equal temperature as the reference cell. The instrument will maintain the temperature of the sample cell by adjusting the power accordingly to the binding event. Integration of the power over time will give the heat change, which is the enthalpy of the reaction [71].

Even though ITC is a powerful technique, its sensitivity requires the thorough design of the experiment and sample preparation. The buffers of the protein sample and the ligand have to be matching as even small discrepancies can affect the experiment in such a way that the readout can not be interpreted correctly.

A critical parameter that will affect the outcome of the ITC experiment is the c value, which determines the binding isotherm of the experiment. The c value is defined as $c = \frac{nPt}{Kd}$ where Pt is the protein concentration, n is the number of binding sites per protein molecule, and K_D is the binding affinity constant. The c-value will affect the shape of the binding curve, which should preferably have a sigmoidal shape and should not be

too steep or too shallow. Therefore, by adjusting the protein and ligand concentration can give a desired c value in the range of 5-1000 [72].

In this work, CbMraY wild-type protein was purified as described in section 2.1.3. The ligands were diluted from stock solutions in DMSO in a SEC buffer that was matching the final protein buffer. Appropriate amounts of DMSO was added to the protein sample to match the DMSO concentration of the ligand samples. All experiments were run in triplicates at 25°C. In order to verify that the buffers of protein and ligand samples were matching, control experiments were performed in advance. The controls were involving the titration of sample buffer into the protein sample and the titration of the ligand into the sample buffer. The control can give information about the background heat, which is generated by the biological system and can be subtracted from the actual experiment.

2.2.4 Water-LOGSY NMR

Water-LOGSY (Water-Ligand Observed via Gradient SpectroscopY) is a sensitive NMR experiment to observe and characterise the binding of a ligand to a macromolecule of interest [73]. The binding experiment is a variant of STD (Saturation Transfer Difference), meaning the source magnetisation is derived from bulk water protons. In this type of experiment, the ligand binding is indirectly observed via NOE (Nuclear Overhauser Effect) [74].

Inhibition of CbMraY by tunicamycin was indirectly observed by the implementation of a competitive ligand binding assay [75] as the signal derived from tunicamycin was not believed to be sufficient. Therefore, purified CbMraY was added to UMP, which acts as a weak inhibitor of MraY. In the next step, tunicamycin is titrated into the sample in order to examine if tunicamycin has the ability to compete out UMP and bind to MraY. In this case, the observed binding derives from UMP.

2.2.5 Thermal stability of MraY

Knowledge about the thermostability of proteins can give valuable information about the physical and chemical processes involved in protein folding. The thermal stability of a protein is usually determined by the thermal unfolding transition midpoint T_m (°C), which is defined as the temperature at which half the protein population is unfolded [76]. During a thermostability experiment, the unfolding process of a protein due to heat is monitored. Addition of chemical additives such as drug compounds can affect the kinetics of protein denaturation and result in a shift of the protein denaturation curve, which represents the heat-induced unfolding process of a protein over time [77]. Thermostability assays are useful tools to characterise membrane protein stability, to compare the quality of different protein samples and to screen for buffers and detergents.

The thermal stability of CbMraY and the effect of selected inhibitors on the heat-induced unfolding was observed with label-free nano DSF, which is a differential scanning fluorimetry technology. The thermal stability is derived by monitoring changes in tryptophan fluorescence present in the protein of interest. As the intrinsic tryptophan fluorescence is depending on the protein structure, thermal unfolding will lead to shifts of fluorescence emission peaks and changes in fluorescence intensity. Thermal unfolding curves are obtained, and T_m of the protein can be calculated from changes in tryptophan fluorescence intensity or the ratio of tryptophan emission at 350nm and 330 nm corresponding from the shift of tryptophan emission due to unfolding of the protein.

For this thesis, purified CbMraY wild-type protein was prepared as described in section 2.1.3. Nano DSF experiments were performed for the apoprotein and in the presence of different inhibitors diluted in protein buffer from stock solutions in DMSO. A control experiment was including apoprotein in the presence of DMSO. Melting curves were obtained via a heat gradient from 25°C - 95°C at 1°C/min using a Prometheus (NanoTemper).

2.3 Protein-ligand docking

Docking experiments have become a powerful tool in structure-based drug discovery. The ability to dock an extensive library of compounds into the active site of a target protein enables a more efficient and less cost-intensive approach in finding potential hits, as fewer compounds need to be tested experimentally. Besides virtual screening of compounds, docking can be used for the prediction of protein-ligand interactions, providing useful information about the active site geometry of a protein-ligand complex [78].

In order to study the ligand interactions of tunicamycin with GPT, the compound has been docked into the active site of apo human GPT (PDB ID: 5LEV). The protein-ligand docking experiment has been performed using the Glide docking and scoring methodology provided by the Schrödinger Maestro software package. The method is based on the "Induced Fit" docking protocol. The scoring functions in Glide rank the ligand poses according to their calculated binding affinity (kcal/mol) [79, 80].

Before the docking experiment can be started, the protein file needs to prepared in Schrödinger, including adding and optimisation of hydrogens, removal of water molecules and assignment of the active site via generation of a grid. In the next step, a 3D structure of the ligand will be generated. Hydrogens are added, and protonation and tautomer states are assigned. Finally, the docking experiment can be initiated.

2.4 Protein Crystallisation

To determine the 3D structure of proteins is of utmost interest for medical applications and the pharmaceutical industry. X-ray crystallography has long been - and still is in most cases - the standard technique in structural biology of proteins. Even though the technique is relatively mature, it relies on the production of pure and homogenous samples to produce high-quality crystals, which remains a major bottleneck in structural biology [81].

In order to initiate protein crystallisation, it is necessary to reach a supersaturated state of the solution that contains the proteins and at the same time, do not disrupt their native states [82]. Supersaturation is achieved by adding mild precipitating agents - such as salt and polymers - and by adjusting the temperature, pH and ionic strength. Despite protein crystallography being an old technique, the experiments are still to a large extent relying on a combination of trial and error and experience, and we are only now starting to explore the physical processes that initiate crystal formation and phase transition [83, 84].

Membrane protein crystallisation The importance of membrane proteins and their challenges in structural biology was mentioned in section 1.4. Due to their hydrophobic nature, membrane proteins are notoriously difficult to work with, and as a consequence, they are underrepresented in the structural protein database PDB [85].

The process of membrane protein crystallisation starts with a large screen of crystallisation reagents that might initiate crystal formation. Advances in the field over the last decade enable automated crystallisation screening using robotics, and commercial kits are available that especially favour crystallisation of membrane proteins [86, 87]. In the event of initial crystal hits, the conditions require further optimisation to obtain well-diffracting crystals.

The use of a lipidic cubic phase (LCP) may be advantageous for the crystallisation of membrane proteins: here the membrane proteins are reconstituted - out of the detergent micelle - into a lipidic cubic phase that enables free diffusion of the proteins in the continuous lipidic cubic phase [88]. LCP mimics the natural environment of membrane proteins as it forms bilayers composed of neutral and native lipids [89].

Chapter 3

Structure-based drug discovery applied to CbMraY

The following section summarises the work performed with the bacterial membrane protein CbMraY, beginning with our complex structure and ending with the biophysical characterisation of modified tunicamycins together with a rationalisation of selective MraY inhibitors.

3.1 The crystal structure of CbMraY

We have solved the crystal structure of CbMraY in complex with the natural product inhibitor tunicamycin [35] as part of this project in 2017 (**Paper I**). A detailed description of the active site with the bound inhibitor is provided in section 3.1.1 and (**Paper I** and **Paper II**); CbMraY numbering is used throughout in section 3 unless stated otherwise. The overall structure of CbMraY is similar to AaMraY; it comprises ten transmembrane helices (TM1-TM10) with both the N terminus and C terminus located on the periplasm, five cytoplasmic loops (loops A, B, C, D and E) and four extracellular loops (Figure 3.1). The periplasmic β-hairpin and the additional periplasmic helix between TM6 and TM7 are incomplete in our structure (in contrast to AaMraY). The glycine residue G258 - conserved throughout the bacterial MraYs - breaks TM9 into two helical segments (TM9a and TM9b), creating a 50° bend at the second half of TM9 relative to the membrane [34–36]. Thus TM9b protrudes 20 Å into

the lipid bilayer. In contrast to the apo AaMraY, CbMraY contains helix 9c (also called the loop-E-helix) consisting of 11 residues located between TM9 and TM10, which is consistent in all available complex structures of MraY.

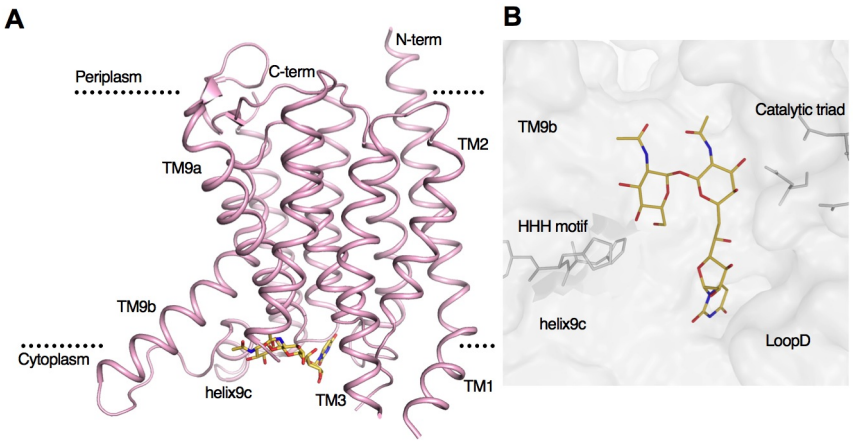

Figure 3.1: Crystal structure of CbMraY. (A) Overall structure of CbMraY (PDB ID: 5JNQ) in complex with tunicamycin (orange). Dotted lines indicate the orientation in the lipid membrane. The figure is based on [90]. (B) Active site view in surface representation with bound tunicamycin. Residues of the catalytic triad and the HHH motif are represented as sticks.

The active site of CbMraY is composed of a cytoplasmic cleft containing several conserved polar and charged amino acid residues (discussed in section 3.1.1). Helix 9c forms one side of the cytoplasmic cleft, which is lined by TM5-TM10 and loops C and D and contains catalytically essential amino acid residues including the aspartic acid triad and the HHH motif [24]. The catalytically active Mg^{2+} ion is absent in the CbMraY structure; in contrast to the apo AaMraY structure, where the Mg^{2+} ion is interacting with D231 (D265 AaMraY). The absence of magnesium in the CbMraY structure is due to the direct interaction of D231

with tunicamycin - it has been shown that tunicamycin is competing with magnesium [36, 37]. Thus even in the presence of Mg^{2+} MraY would be incapable of binding tunicamycin and Mg^{2+} simultaneously [35].

Ligand binding seems to induce significant conformational changes in MraY as shown by the MraY complex structures, which is in stark contrast to the apo AaMraY structure that is lacking a well defined active site. Also, a recently published structure of AaMraY in complex with capuramycin shows that Loop E is disorder - similar to the apo structure - as the compound is not occupying this part of the active site (Mashalidis, 2019); but, different to the apo structure, helix 9c is well defined. In contrast, the apo GPT structures (PDB ID: 5LEV and 6FM9) reveal a well defined active site, which is very similar to the ligand-bound structures (**Paper II**, Section 3.3). The difference between the apo MraY and the complex structures may reveal major conformational changes due to ligand binding or may be a result of crystal packing. Despite missing an apo CbMraY structure, thermal stability measurements with CbMraY seem to indicate bigger structural changes upon tunicamycin binding as well: Figure 3.2 illustrates nano DSF measurements comparing apo and tunicamycin bound CbMraY (unpublished data collected as part of this project). Analysis of the ratio F350nm/330nm reveals, in addition to the thermal shift, a distinct pattern of the melting curves, which distinguishes ligand-bound from the apo structure. It would be interesting to investigate the respective melting curves of apo and tunicamycin bound GPT [38]. These melting curves are expected to show high a similarity between apo and ligand-bound GPT - regardless of the significant thermal shift ($\sim 30°$C [38]).

CbMraY, as seen in all available MraY structures, crystallises as a dimer. The dimerisation interface in CbMraY is comprised of TM1, TM7 and TM10 forming a central hydrophic tunnel with a detergent molecule and a lipid tail bound in our structure (**Paper I, Paper II**). The interface lipids are suggested to play a role in regulation of the enzymatic activity [39, 91].

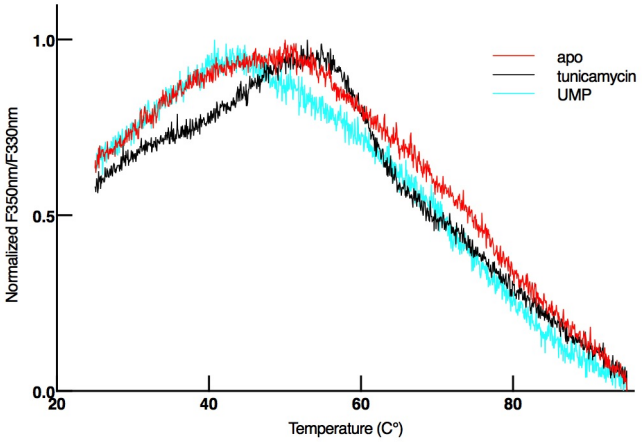

Figure 3.2: Thermal stability of CbMraY. Normalised melting curves of apo CbMraY (red), in complex with tunicamycin (black) and in complex with UMP (cyan).

3.1.1 Active site geometry

Our CbMraY-tunicamycin complex reveals a detailed active site pocket with the bound natural product inhibitor as presented in **Paper I** and **Paper II** (Figure 3.3 provides a ligand interaction map). As described in the previous section, tunicamycin is bound in a wide cytoplasmic cavity, forming interactions with residues F173, G176, N221, F228, N172, D175, D178, D231, H290, H291. The cavity formed by residues G176, N221 and F228 wedges the uracil ring of tunicamycin and N221A and F228A mutants lead to almost complete inactivation of CbMraY. The uracil ring is coordinated by N221, D178 and by L177 via backbone interactions, while the uracil base stacks against F228 via pi-pi interactions. The HHH motif is part of the amphiphilic helix 9c in CbMraY consisting of the residues H290, H291 and H292 - these residues form major interactions with tunicamycin and are conserved among the MraYs [24,92]. The GlcNAc ring of tunicamycin interacts with H291 and stacks against F173 and P288. Our mutations of residue H290 led to almost complete enzyme inactivation. Residue D175 interacts with the 5´-hydroxyl group of tunicamycin, confirmed by our mutational studies showing that D175 is crucial for MraY

activity. The position of the fatty acyl tail of tunicamycin is absent in the CbMraY structure due to poor electron density. However, the interaction of the fatty acid amide in tunicamycin with the residue N173 suggests the fatty acyl tail stretches along TM5 into the membrane, which is further supported by the GPT-tunicamycin structure discussed in section 3.3.

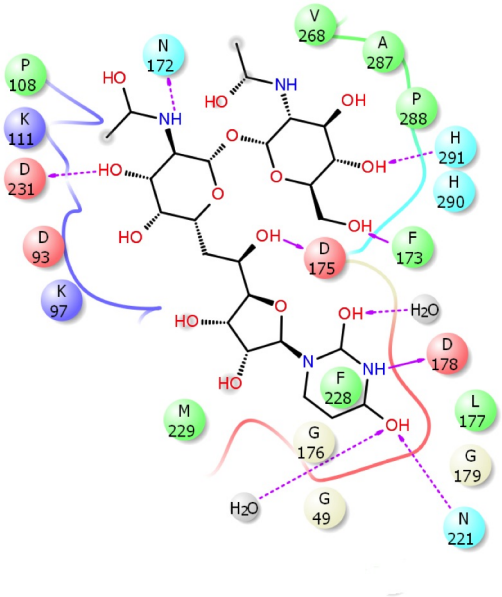

Figure 3.3: Ligand interactions map. Interactions with tunicamycin and CbMraY active site (PDB ID: 5JNQ) as mapped with the ligand interaction map (Maestro, Schrödinger). The illustration is adopted from [35].

3.1.2 Enzymatic activity of CbMraY

To investigate the translocase activity of CbMraY, we performed a FRET-based activity assay on membrane fractions containing overexpressed CbMraY (**Paper I**) and determined the initial rate (2.1×10^4 -ΔF520/min; 5μg/ml total membrane protein concentration) from the single wavelength F520nm

(instead of the ratio F590/F520) as it follows the direct consumption of UDP-MurNAc-pentapeptide, illustrated in Figure 3.4.

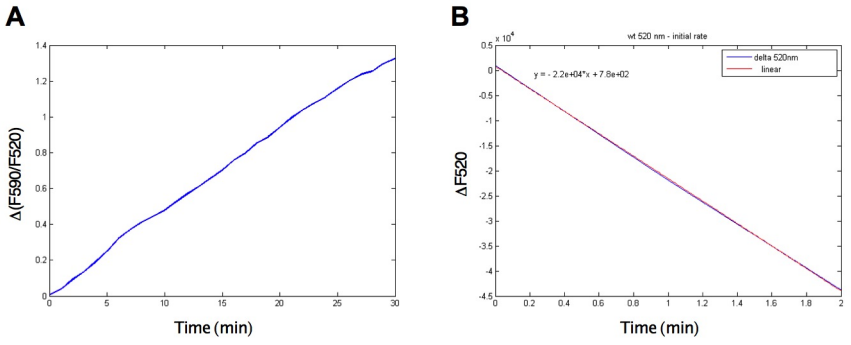

Figure 3.4: Initial rate determination. Determination of initial rate for wild-type CbMraY . 5 μg of membrane fractions were used to obtain linear progress curves for a 30 minutes reaction (A). Initial rates were then calculated from the first two minutes of the ΔF520nm signal (B).

3.1.3 Mutations to probe the active site

Mutations in the active site of CbMraY aided the investigation and speculation of specific residues involved in substrate binding or positioning as summarised in **Paper I**. Figure 3.5 illustrates the progress curves of the respective mutant proteins. The residues F228, N172, D175, D178, D231, H290 and H291 are crucial for MraY translocase activity [92], confirmed by the low enzymatic activity of D175N, D231A and H290N mutant proteins (**Paper I**). In contrast to a BsMraY (*Bacillus subtilis MraY*) mutant N221A (Bs numbering) that showed enzymatic activity [92], our mutants of N221 were almost entirely inactive; thus, N221 is likely involved in substrate binding in CbMraY.

The phenylalanine F228 is conserved among the PNPT family; mutation to alanine led to almost complete inactivation of the enzyme, and docking studies suggest an involvement of this residue in substrate binding (**Paper I**). Mutations of D175 resulted in inactive MraY enzyme - D175 is essential

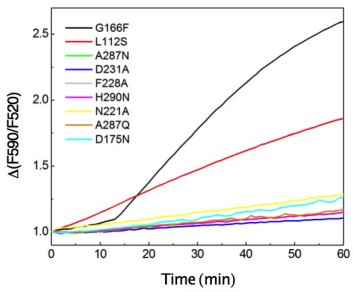

Figure 3.5: Enzymatic activity of CbMraY mutant proteins. Progress curves from the FRET-assay. Concentration of membrane fractions containing overexpressed mutant proteins were adjusted to obtain similar progress curves as for the wild-type protein.

for MraY activity (and conserved in MraYs [92]) as the residue is involved in uracil binding and potential coordination of a metal ion. Hydrophobic mutations of D175 destruct MraY activity; substitution to an asparagine maintained some coordination to the metals but showed reduced affinity to the metal ions and reduced binding of uracil [36].

3.1.4 Binding modes of the natural product inhibitors

The natural nucleoside antibiotics share a common uridine motif - which is also present in UDP-MurNAc-pentapeptide - and only tunicamycin and mureidomycin interact with the residue D231 responsible for Mg^{2+} binding, and both inhibitors compete with the magnesium ion, as shown previously [36, 37]. Analysis of all available complex structures reveal that the uridine motifs are wedged in the uracil binding pocket with almost entirely overlapping conformations for the inhibitors [37] (see Figure 3.6, the natural product inhibitors are superimposed in the CbMraY active site). Interestingly - among the natural nucleoside inhibitors - only tunicamycin shows cross-reactivity with GPT. Despite similar binding modes of the uridine motifs, the uracil binding pocket allows some degree of flexibility as highlighted in **Paper II** and shown in the slightly different binding modes for capuramycin and 3-hydroxymureidomycin A.

In contrast to the structural similarity of the uridine motifs in the uracil pocket, the adjacent pocket lined by residues T52, N172, D175, and G230 (AaMraY numbering) allows binding of different motifs, while maintaining

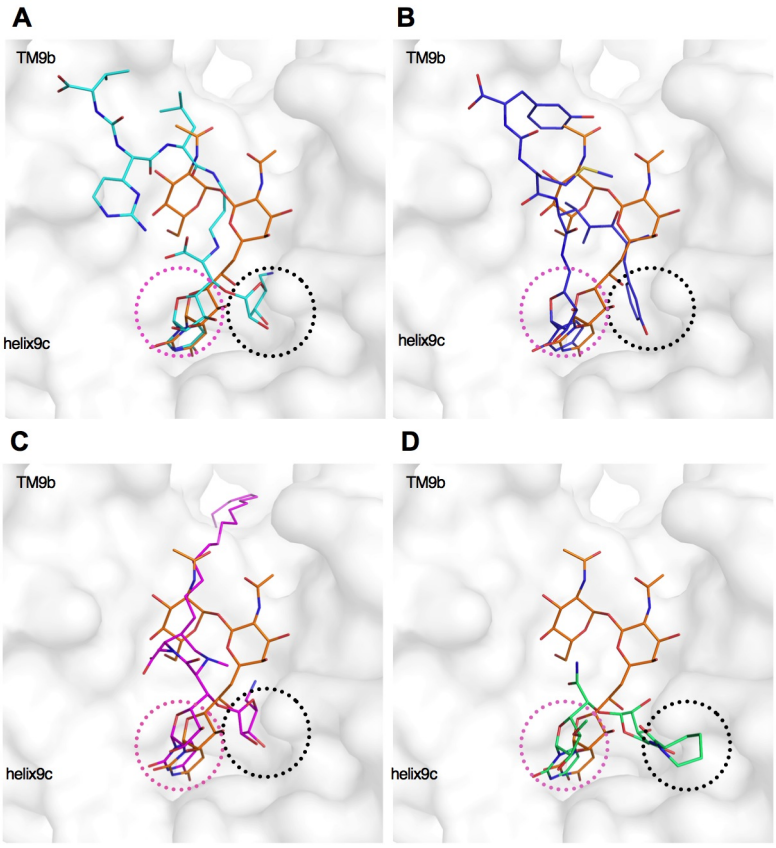

Figure 3.6: Structures of the MraY nucleoside inhibitors. Comparison of the nucleoside inhibitors in the active site of CbMraY (PDB ID: 5JNQ). Tunicamycin (orange) is superimposed with the inhibitors: (A) MD2 (PDB ID: 5CKR) (B) 3´-hydroxymureidomycin A (PDB ID: 6OZ6) (C) Carbacaprazamycin (PDB ID: 6OYH) (D) Capuramycin (PDB ID: 6OYZ). Circles in pink highlight the uracil binding pocket; circles in black the uracil adjacent pocket.

a similar orientation of the active site residues [37]. Compared to the other nucleoside inhibitors, tunicamycin is missing hydrogen bonds with the residues of this pocket, but instead forms hydrogens bonds with K111 and backbone interactions with F173.

3.2 Novel and optimised protocols for purification of membrane proteins

Even though we could solve the structure of CbMraY in complex with tunicamycin, low expression levels and yield and low stability of the purified protein hampered the ongoing project. To further investigate the binding of tunicamycin and modified tunicamycins via biophysical techniques, the existing protocol required optimisation as described in the next section.

3.2.1 Optimisation of CbMraY expression, purification and crystallisation

Improved protocol for expression and purification To overcome low yields and low stability of the purified CbMraY, we adjusted the expression protocol by slowing down expression and delayed the induction via the addition of glucose to the cultures. This simple alteration led to an improved yield of correctly inserted membrane protein by a factor of $\sim$15 compared to the previous protocol. Besides, we modified the purification protocol, so that no membrane preparation step is required and the membrane proteins are extracted directly from the crude cell lysate with the detergent DDM that is exchanged during IMAC to DM. The final protocol provided larger amounts of stable membrane proteins for subsequent use in biophysical assays such as ITC, which require high amounts of sample (**Paper III**).

Crystallisation All available structures of the PNPT superfamily, including our in-house structure, are of modest resolution. The solvent content is high, the crystal packing is poor, and all structures have derived from vapour diffusion experiments. To improve crystallisation of CbMraY, we continued working with the same construct and obtained initial crystal leads in different conditions as shown in Figure 3.8 (no crystals could be obtained in the original conditions), which are reproducible. Furthermore, detergent effects [93] may also limit the resolution. For future studies, we, therefore, would like to perform detergent screens to overcome this issue. Besides, we attempted to establish a protocol for the crystallisation of MraY in LCP, but large screens resulted in poorly diffracting hits.

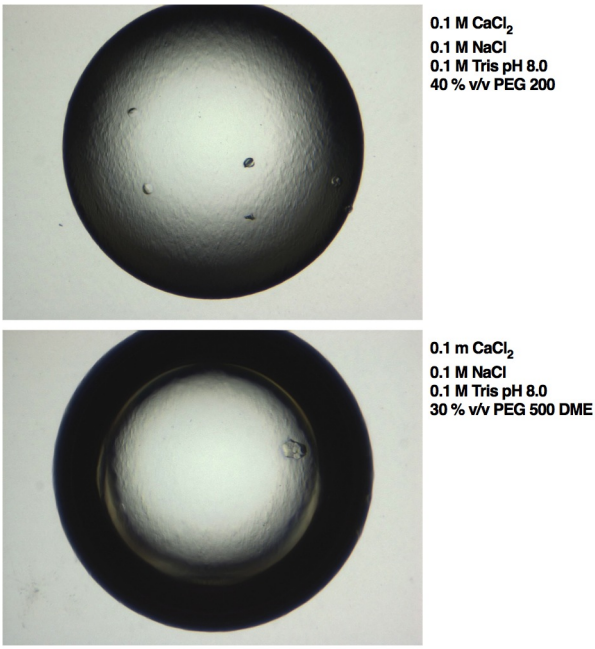

Figure 3.7: Crystallisation screen of CbMraY. Obtained crystals of CbMraY in complex with tunicamycin.

Furthermore, for future studies, we would like to design novel CbMraY constructs aimed at adding a fusion tag (BRIL) on the N-terminus; thereby increasing opportunities for crystal contact formation.

3.2.2 A new protocol for improved membrane protein purification using teabags

We chose the teabag system to investigate its value in membrane protein purification (see detailed description in **Paper IV**) and [94]. We have purified different membrane protein targets with the teabags and compared the samples to the conventionally purified proteins. Briefly, teabags can be prepared from a nylon mesh using varying sizes and filled with an affinity resin of choice. After heat-sealing and a washing step, the teabags can be either stored in ethanol or used directly for protein purification [94].

Despite advances in the field, membrane protein production and purification remain challenging, demonstrated by the underrepresented crystal structures deposited in the protein database PDB [95]. As described in **Paper IV**, our novel method allows purification of membrane proteins cheaply and easily, with significantly reduced purification time. In our study, membrane proteins purified with teabags were stable and of high quality, which we used for subsequent structural and functional studies. We could demonstrate a better purity and quality of the teabag samples: in general, elution peaks from the size exclusion profiles appeared sharper from the teabag samples. Electron microscopy of our test protein (the chloride ion channel CIC-1) revealed that teabag samples were more homogenous compared to the conventionally purified protein.

We hypothesised the better quality of the teabag samples derives from milder purification conditions: no pressure applies on proteins due to the lack of columns or automated HPLC systems, the shorter purification time reduces the exposure time to the high concentration of the solubilising detergent, and the teabag samples might be less delipidated due to the shorter purification time [96].

The strengths of our study are the use of different membrane proteins - including pharmacological relevant and challenging targets - covering different expression systems, detergents and IMAC resins. We could demonstrate that teabag purification significantly reduces the purification time while allowing the production of pure samples of high quality. The use of teabag purification may be advantageous for purification of challenging membrane proteins (**Paper IV**).

3.3 Cross-reactivity with human GPT

As mentioned in section 1.5, the eukaryotic PNPT family member GPT is a structural homolog of the bacterial MraYs and targeted by tunicamycin. Hence, tunicamycin is toxic to humans and preventing its usage as an antibiotic. Our complex structure and biophysical characterisation

of CbMraY and tunicamycin together with the release of the GPT structures [38, 39] enabled a thorough structural comparison with the bacterial MraYs - leading the way to the rationalised compound design of antibiotics that selectively target MraY (**Paper II** and **Paper III**).

3.3.1 Structural comparison of MraY and GPT

The overall fold of human GPT is similar to MraY and comprises ten transmembrane helices, with both the N-terminus and C-terminus located luminal, and four extracellular and five cytosolic loops. Besides the missing cytosolic doming in MraY, including the $\beta\alpha\beta\beta$ motif, the overall structure of human GPT appears similar to MraYs with mostly overlapping, transmembrane helices, including the active site (Figures 3.8 and 3.9). The cytosolic domain of GPT is protruding into the active site, making it more restricted. The C-terminal ending of helix 9b is not entirely overlapping with the corresponding helix 9b of MraY, as it is tilting more inwards so that the ending side chains L293/294 of helix 9 are protruding, pointing towards the active site. Human GPT provides a complete structure compared to MraY, where missing loops are connecting the transmembrane helices in MraY - the uridine binding motif / β-hairpin motif is not visible in the MraY structures [39] (**Paper II**).

3.3.2 Active site comparison

The active site of GPT appears more narrow and closed up compared to CbMraY. It is worth to mention that a comparison of the active sites could result in a somewhat misleading picture of the MraY active site - not all loops were modelled to due poor resolution. Helix 9c - lined by loops 5-6, 7-8 and helices 5-10 - and the additional cytosolic domain form the cytoplasmic cleft. The uracil binding pocket is slightly bigger in GPT. Due to changes in the 9b-c stretch, the additional loop is protruding towards the active site; making it more narrow and less accessible than the shallow active site in CbMraY. The C-terminal ending of helix 9b is slightly tilted compared to CbMraY so that the ending residues are protruding towards the active site. This region is the cavity for the fatty acyl chain of the substrate and tunicamycin. In the GPT-tunicamycin complex structure

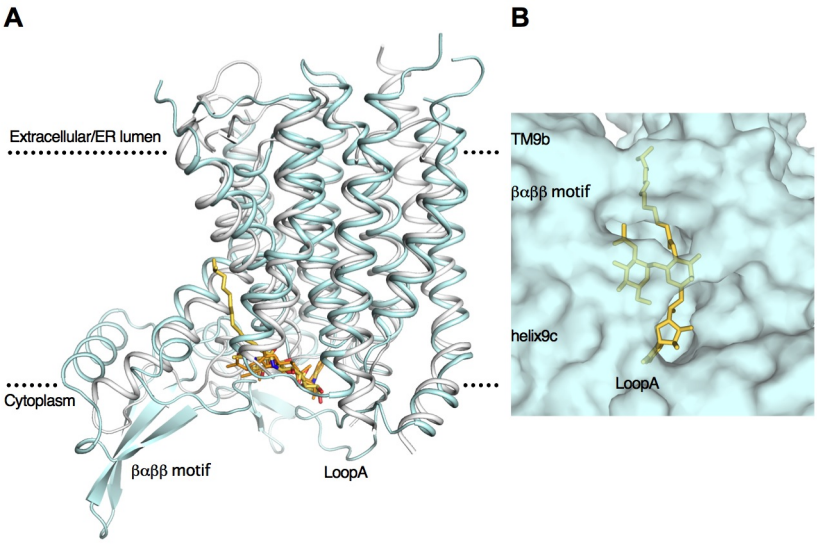

Figure 3.8: Structural comparison of GPT and MraY. (A) The CbMraY(white)-tunicamycin complex (PDB ID: 5JNQ) superimposed with the human GPT(cyan)-tunicamycin complex (PDB ID: 6BW5). Orientation within the lipid membrane is indicated by dashed lines. The figure is modified from [90] (B) Acite site view in surface respresentation of GPT with the bound inhibitor tunicamycin (yellow). Transparency of the surface visualizes tunicamycin is enclosed in the GPT active site.

and the residues W122, H302 and R301 (all GPT numbering) are flipping down locking the bound tunicamycin in place. The movement of W122 creates a narrow tunnel to position the fatty acyl chain of tunicamycin. The movement of the sidechains H302 and R301 closes the cavity in which the nucleoside is bound to even tighter. Figure 3.9 illustrates interactions with tunicamycin [39] (**Paper II**).

The following paragraph discusses the use of ligand docking to analyse the interactions of human GPT and tunicamycin, which we conducted before the release of the GPT-tunicamycin complex [39] (see section 2.3 for experimental design of the docking). Figure 3.9 shows an alignment of the active sites of the docked complex and the published GPT-complex

structure: we determined likely interactions of tunicamycin with human GPT with the best docking pose (most similar to the tunicamycin conformation in the CbMraY structure) including the residues R301, H302 and R303 (GPT numbering), which are essential for GPT activity [91]. The

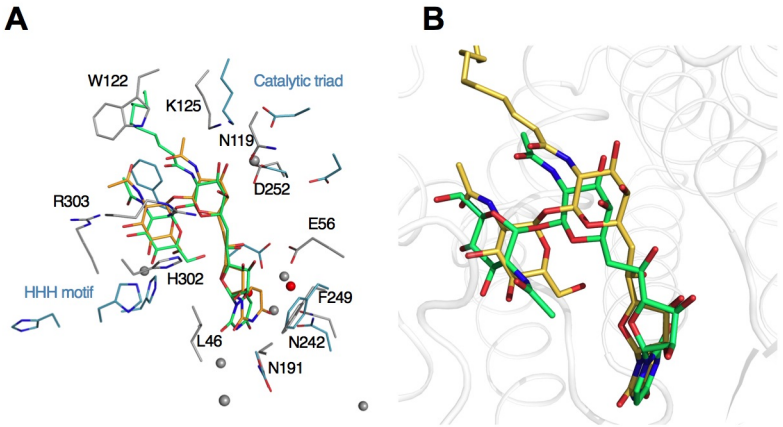

Figure 3.9: GPT active site interactions.(A) Active site comparison of CbMraY (blue)–tunicamycin (yellow) complex (PDB ID: 5JNQ) superimposed with the GPT (white)– tunicamycin (green) complex (PDB ID: 6BW5). Residues that interact with the ligands are shown as sticks (GPT numbering). (B) Comparison of the docked pose of GPT (not visualised) and tunicamycin (green) superimposed with the GPT (white)-tunicamycin (yellow) complex (PDB ID: 6BW5).

docking proposed interaction with L293 pointing towards the GPT active site - which is missing in MraY - and the stacking with F249 in the uracil binding pocket. The docking suggested more direct interactions with tunicamycin compared to the CbMraY structure, which is in agreement with the published structure [39]. Despite the docking was performed with an apo structure, and tunicamycin being a problematic compound to use in docking due to flexibility of the ligand structure, the experiment was successful.

The resulting pose was similar to the crystal structure and predicted most interactions of the active site residues with tunicamycin. The use of

ligand docking is therefore recommended in cases where a 3D structure is missing. It is worth to mention that the docking was successful since the apo and GPT complex structures show a high similarity and the complex structure of MraY with tunicamycin was available to aid in the assignment of the docking poses.

3.3.3 Comparison of tunicamycin interactions

In GPT, both the uracil and the ribose ring position in a small cavity where the two of them form interactions with side chains of the active site, and the pocket appears more prominent than in MraY. In CbMraY, only the uracil ring interacts with the active site residues. Modifications of the ribose ring could lower the affinity for GPT, but the affinity for MraY may be unaltered.

The 6-bis-hydroxyl group of GlcNAc forms no interactions with GPT, whereas it interacts with F173 in MraY. Therefore, removing the 6-bis - hydroxyl group, as in QVM (**Paper III**), could lower the affinity for MraY, but it should not affect the affinity for GPT - as confirmed in Paper III and [53].

In contrast to MraY, both the 3-bis-hydroxyl and the *N*-acetyl group interact with R303 in GPT. Modifications of this motif in tunicamycin would probably show no effect in MraY but may lower the affinity for GPT. Residue R301 coordinates the oxygen in the tunicamine sugar ring in GPT. In contrast, this oxygen is not involved in interactions with the MraY active site amino acids. Modifications at this part of the tunicamine - to disrupt interactions with R301 - could lower the affinity for GPT, whereas the affinity for MraY may remain unaltered. In contrast to MraY, no interactions with the 5'-hydroxyl group in GPT are present due to the lack of a corresponding aspartic acid in this region of GPT.

3.4 Biophysical characterisation of tunicamycin binding

In this project, a competitive 1D-NMR binding assay led to the first investigation of the direct binding of tunicamycin to purified CbMraY wild-type protein using UMP as a weak inhibitor. Figure 3.10 shows the setup of the experiment: The experiment is initiated with the inhibitor UMP in assay buffer. Addition of purified CbMraY leads to binding of UMP to MraY that is competed out by addition of tunicamycin in a following step. Despite the success of this experiment, we decided to determine the binding constant K_D with alternative methods, as the difference in potency between tunicamycin and UMP was expected to be too large for an accurate determination of the dissociation constant. This assumption may be false due to our inhibition measurements with UMP and MraY (IC_{50}: 20000 nM) as described in the following paragraph.

Further investigation of the inhibition of CbMraY with the FRET-assay allowed determination of the IC_{50} for tunicamycin (391nM, Figure 3.11), reflecting the inhibitory effect on MraY present in membranes and not purified protein, which is in agreement with previous studies performed with AaMraY (450nM IC_{50}, [39]). We performed ITC experiments to determine the K_D value (233nM), which was in the same range as in studies performed with AaMraY [39]. Used as a control compound, UMP showed inhibitory effect on CbMraY with an IC_{50} of 19.500nM.

3.4.1 Modified tunicamycin analogues and their binding to MraY

In order to find potent and selective MraY inhibitors, we investigated structural motifs of modified and purified tunicamycins to rationalise inhibitory effects as determined by half-maximal inhibitory concentrations (IC_{50}), binding affinities and thermal stabilities (**Paper III**). To do so, we have altered four parts of the tunicamycin motif: the length and branching of the fatty acyl chain, the saturation of the fatty acyl chain, the 6-bis-hydroxyl group of the GlcNAc ring, and the ring structure of the uracil motif.

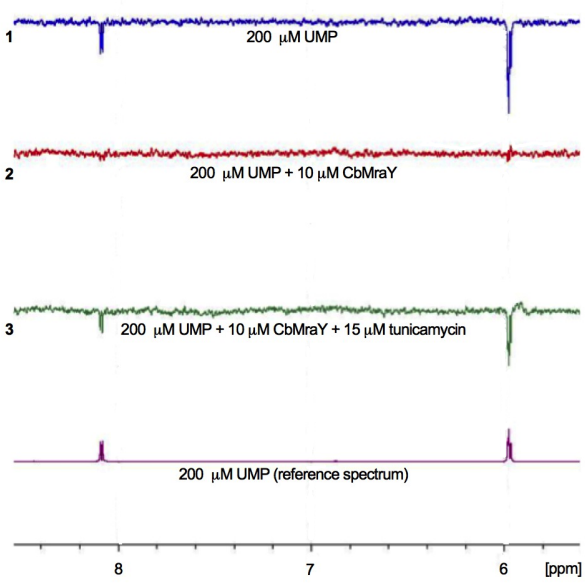

Figure 3.10: Tunicamycin binding to CbMraY by 1D NMR. Competitive ligand binding with tunicamycin and UMP. 1, the upper trace used as a reference step to rule out that UMP does not form interactions with detergent micelles; 2, the next lower trace visualises UMP binding to CbMraY, which is competed out in the next step (3) by addition of tunicamycin. The lower trace (4) illustrates a UMP reference spectrum.

Tunicamycin consists of different variants where the end of the fatty acyl chain occurs in different configurations including iso (CH3CH(CH3)-), anteiso (CH3CH2CH(CH3)-) and unbranched (CH3CH2-) [97], and can vary in length (illustrated in Figure 3.12). A purified tunicamycin anteiso analog has not been observed and reported before, but has been reported for streptovirudins and corynetoxins [52]. We investigated the inhibitory effect for purified tunicamycins with varying chain lengths (Tun14:1-17:1). Our findings demonstrate a high potency for the shorter chain length compounds with an optimal chain length of 15:1(iso) followed by 16:1(iso) and 17:1(iso) (Figure 3.13). Interestingly, Tun14:1(iso) showed reduced potency, lower than 17:1(iso).

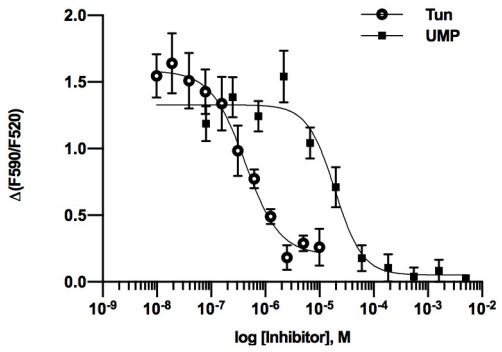

Figure 3.11: Inhibitory effect of tunicamycin. IC_{50} plots showing the inhibitory effect of tunicamycin and UMP.

Also, the branching type had an impact on inhibition and potency, as shown by the increased values by approximately 8-fold of the anteiso compounds compared to their iso branching counterparts. Figure 3.13 shows IC_{50} plots, ITC binding isothermals and melting curves. It is worth to mention that we observed the same potency trend in all assays. The location of the branching seems to impact the inhibitory effect against MraY, demonstrating the importance to have maximal interactions between the inhibitor and the active site residues.

Reasoning, how the branching and the length of the fatty acyl chain impact inhibition and potency towards MraY, is hampered by the lack of electron density in the MraY structures. Both the CbMraY-tunicamycin complex and the MraY-carbacaprazamycin complex show poor density for the fatty acyl chain; thus rationalisation of the branching position based on the structures could be problematic. Nevertheless, an inspection of the carbacaprazamycin fatty acyl chain opens up room for speculations: we have superimposed the MraY-carbacaprazamycin complex and the GPT-tunicamycin complex (PDB ID: 6BW5) in the active site of CbMraY. A phenylalanine F162 in the hydrophobic tunnel would prevent tunicamycin from binding to MraY similarly as in GPT so that the fatty acyl chain

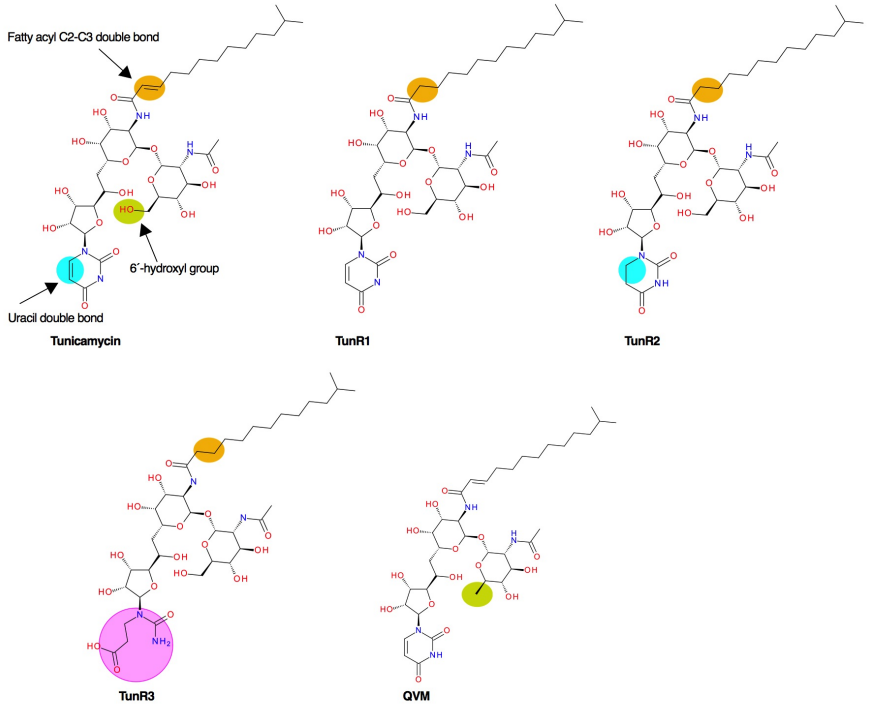

Figure 3.12: Chemical structure of modified tunicamycins. The modifcations are illustrated in comparison to the core structure of tunicamycin. TunR1, TunR2 and TunR3 are a mixture of the N-acyl variants C-14, C-15, C-16 and C-17. QVM is a purified analog of the N-acyl variant C-16.

is forced to make a bend as seen for carbacaprazamycin, where the bent chain is leading towards a restricted pocket (Figure 3.14). In this case, a Tun 14:1 (iso) may be somewhat sterically hindered by F162, in contrast to a Tun 15:1 (iso) having more space in the cavity of the hydrophobic pocket of MraY. The longer chain analogues Tun 16:1 (iso) and Tun 17:1 (iso) may be positioned too close to the restricted pocket and F162 in comparison to Tun 15:1 (iso). According to this reasoning, Tun 15:1 (iso) may fit in the best pose with the fewest steric clashes. Figure 3.14 further illustrates the possible positioning of the Tun 15:1 (anteiso) analogue, where a clash or steric hindrance may occur due to proximity to F162, and

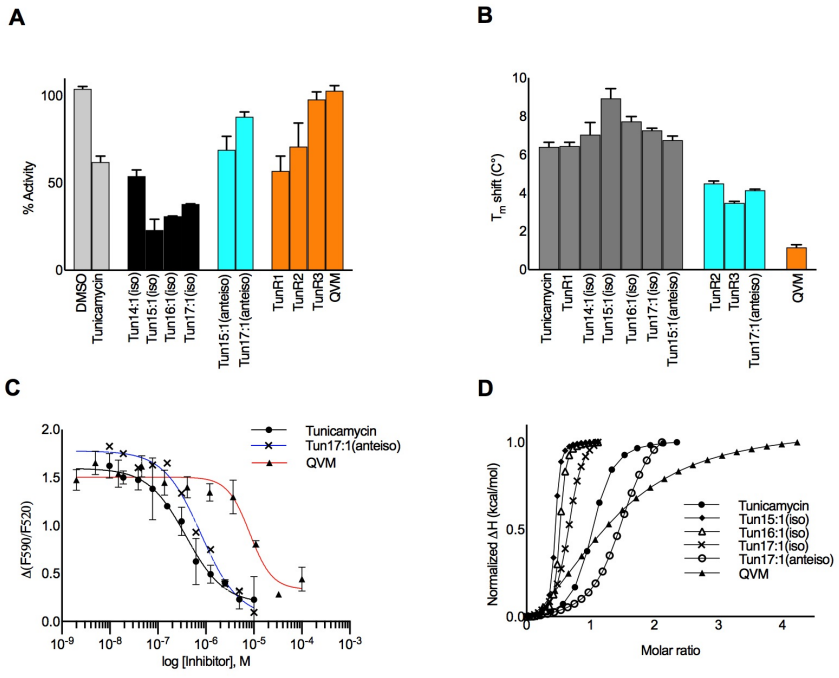

Figure 3.13: Effects of tunicamycin analogs on CbMraY activity and stability.(A) Inhibitory effects of the analogs on CbMraY enzymatic activity as determined by the FRET assay. (B) Effects on thermal stability of CbMraY by the tunicamycin analogs. (C) Dose-response curves from the FRET assay. (D) ITC titration, fitted curves of tunicamycin analogs. Inhibitors were titrated to purified CbMraY protein in the absence of $MgCl_2$.

Tun 17:1 (anteiso) possibly being positioned too close to the restricted pocket and F162. This reasoning may explain the lower potency of the anteiso analogues compared to their iso counterparts.

The purified tunicamycin (iso) analogues showed a higher potency and inhibition compared to commercial tunicamycin. To rationalise this discrepancy, we analysed the commercial tunicamycin sample with 1D NMR to determine the branching types of the acyl chains present in the mixture of homologues. The sample contained iso branching analogues as major

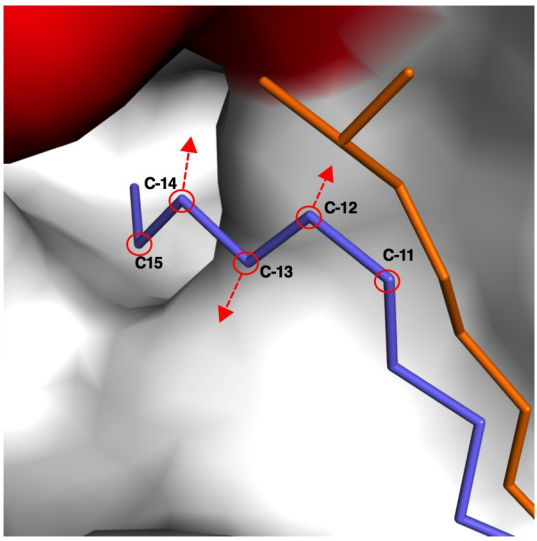

Figure 3.14: Potency of the acyl chain analogues. Comparison of acyl chains of capacrapazamycin (PDB ID 6OYH, blue) and tunicamycin (PDB ID: 6BW5, orange). The two compounds are superimposed in the active site of CbMraY. Numbering of the chain from C-11 to C-15 is highlighted for cabacrapazamycin and red arrows at positions C-12 and C-13 indicate the possible position of the methyl groups for a 14(iso) and 15(iso). F162 is highlighted in red.

component, and a minor fraction of anteiso analogues was present as well. We could not detect an unbranched variant.

TunR1 contains a saturated C2-C3 bond in the fatty acyl chain (Figure 3.12) and showed unaltered inhibitory effect, binding affinity and stabilising effect compared to tunicamycin - suggesting the hydrophobic tunnel in MraY being more adaptable to changes in the C2-C3 bond of the fatty acyl chain. In contrast, GPT contains a more enclosed hydrophobic tunnel, including a tryptophane W122, which locks the lipid tail in place. Thus, GPT is likely more sensitive to alterations in the C2-C3 bond - in agreement with recent studies showing similar inhibition of tunicamycin and TunR1, whereas TunR1 showed reduced inhibition towards *S. cerevisiae* [48].

We investigated the effect of a reduced uracil ring in the modified tunicamycin TunR2, which showed a minor reduction in inhibitory effect and binding affinity by a factor of approximately 1.5-2.0. The uracil group of tunicamycin wedges in a well-defined pocket, where a phenylalanine F228 (conserved in MraYs and GPT) stacks against the uracil ring. Hence, reducing the double bond of the uracil ring likely disrupts the planarity of the uracil ring and influences the pi-pi stacking. The impact on the potency by alteration of the uracil ring was neglectable, which is in agreement with previous studies of streptovirudins [52]. In contrast, TunR2 showed a more reduced potency towards GPT [48,49], where the uracil binding pocket is more rigid compared to MraY.

Investigation of the modified tunicamycin TunR3 (with an open uracil ring motif) revealed a significantly reduced inhibitory effect and binding affinity compared to tunicamycin, which is in agreement with previous studies demonstrating that TunR3 had no inhibitory effect on *N*-glycosylation [50]. In TunR3, the open uracil ring structure likely disrupts major interactions with the uracil binding pocket that occur with the closed uracil ring motif, but must still enable some interactions with the uracil binding pocket. Previous studies found the uracil motif required for inhibition of a modified tunicamycin, where removal of the uracil motif prevented the compound from inhibiting MraY [98].

In the CbMraY structure, the 6´´-hydroxyl group of tunicamycin forms interactions with the backbone of F173 and with the side chain of H290. The missing 6´´-hydroxyl group in QVM likely disrupts these interactions - in agreement with our findings, which revealed a dramatically reduced inhibitory effect and binding affinity of QVM16:1(iso); the IC_{50} and K_D values were approximately 150 times reduced compared to the Tun16:1(iso) analogue. The 6´´-hydroxyl group has a more significant impact on inhibition of MraY compared to GPT as shown by studies demonstrating similar minimum inhibitory concentration (MIC) values of QVM and tunicamycin against *S. cerevisiae*. In contrast, tunicamycin is tenfold more potent than QVM against *Bacillus subtilis* bacteria [53]. This observation

can be explained by the complex structure of GPT and tunicamycin, revealing no interaction of the 6´´-hydroxyl group in tunicamycin and the active site residues of GPT. Furthermore, this is likely the only interaction between the GlcNAc motif and the MraY active site (**Paper I** and **Paper II**), and disruption of this interaction causes dramatic inhibitory changes. This notion is in agreement with a recent study, where the entire GlcNAc motif was removed, resulting in a similar inhibitory effect as QVM in our study [98].

3.5 Rationalisation of selective MraY inhibitors

The release of our CbMraY-tunicamycin complex, followed by the GPT crystal structures [38, 39] led the way to a rationalised approach for the design of selective MraY inhibitors. Despite the similar overall structure, the active site of human GPT shows some distinct differences upon thorough analysis. The most noticeable difference is the enclosed active site of GPT with a more restricted entrance compared to MraY. This simple fact most likely prevents large or rigid compounds from binding effectively to GPT. Furthermore, the overall structure of GPT appears more rigid and ordered, with only minor conformational changes of some active site residues upon ligand binding [39]. Tunicamycin is, therefore, a more potent inhibitor of GPT than MraY (in agreement with published IC_{50} and K_D values: [39]; **Paper III**), and GPT is likely more sensitive to modifications in the binding motifs of the inhibitors. This notion is in contrast to MraY, showing a disordered active site in the apo structure compared to the complex structures - possibly allowing more flexibility to compound binding, as demonstrated in the recently published complex structures (described in section 3.1 and [37]). It is worth to mention that studies suggest a possible complex formation of MraY with the membrane-associated protein MurG [99]. Such a potential complex might change the active site of MraY dramatically, possibly making it more enclosed, similar to GPT.

We found a region of interest in the MraY structure upon reasoning why the natural product antibiotic MD2 is selectively targeting MraY and not GPT. Our structural alignment (**Paper II**) revealed a major clash between

the peptidic moiety of MD2 and the additional cytosolic domain TM9b-TM10; thus preventing MD2 from binding effectively to GPT. This notion is in agreement with a recent study, where substitution of the MurNAc sugar by a GlcNAc sugar reduced the inhibitory effect of a modified tunicamycin analogue towards GPT - rationalised by the active site and sugar substrate differences of MraY and GPT [39].

Observation of the hydrophobic tunnel in the GPT active site pinpoints another region of interest: the hydrophobic tunnel is tighter compared to in MraY, containing W122 (GPT numbering), which locks the lipid tail of the substrate and tunicamycin in place. In **Paper III** we rationalised that due to the restricted tunnel in GPT, alteration of the C2-C3 bond in the fatty acyl chain of tunicamycin has a more significant impact on GPT inhibition without affecting the potency towards MraY. Recent studies picked up on this notion and introduced a second acyl chain to the tunicamycin motif, resulting in a selectively potent compound, which cannot inhibit GPT [38].

Very recently, Lee and coworkers [37] highlighted the binding pocket formed by residues T52, N172, D175, and G230 (AaMraY numbering) - adjacent to the uracil binding pocket - as an exciting site to investigate for selective MraY inhibitors. A corresponding binding pocket is missing in the GPT structure, and it allows binding to a variety of structural motifs (see Figure 3.6). This region in the MraY active site is not a required motif for inhibition but can alter the potency without facing cross-reactivity issues with GPT [37], which is in agreement with previous SAR studies [100,101].

Finally, the uracil binding pocket reveals another region of interest as the pocket appears more well-defined in MraY compared to in GPT. Reduction of the uracil ring in tunicamycin only showed a minor impact on MraY inhibition, whereas potency towards GPT seems to be altered more pronounced, as demonstrated by cell toxicity assays [48]. TunR2 is, therefore, a promising starting compound for the design of selective tunicamycin inhibitors. The following alterations could optimise TunR2 towards a selective MraY inhibitor: use of the higher potency for the shorter chain length tunicamycins, where a TunR2 15:1(iso) should hypothetically be

most potent towards MraY and at the same time further reduce the potency towards GPT; and secondly, reduction of the C2-C3 bond of the acyl chain could further reduce GPT inhibition.

Chapter 4

Concluding remarks

Antibiotic resistance is rapidly growing and considered one of the biggest threats to human health. It is of utmost importance to design and develop novel antibacterial agents in order to slow down antibiotic resistance. The work performed in this thesis involves the structural and functional studies of the antibacterial target MraY with different inhibitors for the future design of antibacterial drugs.

We present the crystal structure of MraY from the pathogen *Clostridium bolteae* in complex with the natural nucleoside inhibitor tunicamycin in **Paper I**. The structure together with functional and biophysical studies of active site mutant proteins provided the detailed binding mode of tunicamycin and substrate binding. Both AaMraY and CbMraY were shown to crystallise as dimers. However, the impact of the oligomeric status on MraY activity remains unclear. Electron density for AaMraY indicated the positioning of lipid molecules in the hydrophic tunnel of the dimerisation interface [34]. Furthermore, MraY enzymatic activity and functional folding was depending on anionic charged lipids and the absence of detergents in the Gram-negative homologues, whereas lipids were nonessential for activity of the Gram-positive BsMraY homologue that tolerated the presence of detergents [102]. This might indicate that the oligomeric status and its impact on MraY activity is different between the Gram-positive and Gram-negative homologues and would be an interesting topic for future investigations.

Our structural comparison between MraY and its human homologue GPT is presented in **Paper II**, where we highlight regions of interest for modifications of tunicamycin to selectively target MraY.

We have modified and purified tunicamycins and investigated their potential for MraY inhibition and potency. Our results, presented in **Paper III**, identified potent MraY inhibitors with reduced toxicity in eukaryotes that may be used for the future design of novel antibacterial drugs. Future studies with GPT and our selected compounds should be performed to examine their inhibitory effect and potency. To investigate the difference in potency and inhibition between the iso and anteiso branched tunicamycins, future studies should aim to crystallise MraY in complex with the different branching variants of tunicamycin.

In **Paper IV**, we have applied the novel teabag method to investigate its use in membrane protein purification. We found that our novel method significantly reduced the purification time, while producing stable and pure proteins that were used for subsequent functional and structural studies. The quality and purity of the teabag samples were identical - or in some cases exceeding - compared to the conventional method. We speculated the exceeding quality of the teabag samples might be related to the shorter purification time resulting in less delipidated samples due to the slow kinetics of delipidation [96], which should be investigated in future studies.

Bibliography

[1] S. B. Zaman, M. A. Hussain, R. Nye, V. Mehta, K. T. Mamun, and N. Hossain, "A Review on Antibiotic Resistance: Alarm Bells are Ringing," *Cureus*, vol. 9, p. e1403, June 2017.

[2] G. A. Durand, D. Raoult, and G. Dubourg, "Antibiotic discovery: history, methods and perspectives," *Int. J. Antimicrob. Agents*, vol. 53, pp. 371–382, Apr. 2019.

[3] E.-M. Antão and C. Wagner-Ahlfs, "[Antibiotic resistance : A challenge for society]," *Bundesgesundheitsblatt Gesundheitsforschung Gesundheitsschutz*, vol. 61, pp. 499–506, May 2018.

[4] B. Malik and S. Bhattacharyya, "Antibiotic drug-resistance as a complex system driven by socio-economic growth and antibiotic misuse," *Sci Rep*, vol. 9, July 2019.

[5] W. H. O. (WHO), "WHO | Antimicrobial resistance: global report on surveillance 2014."

[6] C. Walsh, "Antibiotics: actions, origins, resistance.," *Antibiotics: actions, origins, resistance.*, 2003.

[7] R. J. Melander, D. V. Zurawski, and C. Melander, "Narrow-spectrum antibacterial agents," *Medchemcomm*, vol. 9, pp. 12–21, Nov. 2017.

[8] G. D. Wright, "Q&A: Antibiotic resistance: where does it come from and what can we do about it?," *BMC Biol*, vol. 8, p. 123, Sept. 2010.

[9] K. P. Talaro, *Foundations in microbiology*. Boston: McGraw-Hill Higher Education, 7th ed., [international student ed.]. ed., 2009. Open Library ID: OL27039639M.

[10] D. van Duin and D. Paterson, "Multidrug Resistant Bacteria in the Community: Trends and Lessons Learned," *Infect Dis Clin North Am*, vol. 30, pp. 377–390, June 2016.

[11] T. J. Silhavy, D. Kahne, and S. Walker, "The Bacterial Cell Envelope," *Cold Spring Harb Perspect Biol*, vol. 2, May 2010.

[12] A. Varki, R. D. Cummings, J. D. Esko, H. H. Freeze, P. Stanley, C. R. Bertozzi, G. W. Hart, and M. E. Etzler, eds., *Essentials of Glycobiology*. Cold Spring Harbor (NY): Cold Spring Harbor Laboratory Press, 2nd ed., 2009.

[13] L. Woodward and J. H. Naismith, "Bacterial polysaccharide synthesis and export," *Curr. Opin. Struct. Biol.*, vol. 40, pp. 81–88, 2016.

[14] H. Nothaft and C. M. Szymanski, "Protein glycosylation in bacteria: sweeter than ever," *Nat. Rev. Microbiol.*, vol. 8, pp. 765–778, Nov. 2010.

[15] M. Jankute, J. A. G. Cox, J. Harrison, and G. S. Besra, "Assembly of the Mycobacterial Cell Wall," *Annu. Rev. Microbiol.*, vol. 69, pp. 405–423, 2015.

[16] J. E. Sykes, "Chapter 39 - Cell Wall–Deficient Bacterial Infections," in *Canine and Feline Infectious Diseases* (J. E. Sykes, ed.), pp. 380–381, Saint Louis: W.B. Saunders, Jan. 2014.

[17] Y. Liu and E. Breukink, "The Membrane Steps of Bacterial Cell Wall Synthesis as Antibiotic Targets," *Antibiotics*, vol. 5, p. 28, Aug. 2016.

[18] S. J. Singer and G. L. Nicolson, "The fluid mosaic model of the structure of cell membranes," *Science*, vol. 175, pp. 720–731, Feb. 1972.

[19] H. Watson, "Biological membranes," *Essays Biochem*, vol. 59, pp. 43–69, Nov. 2015.

[20] K. R. Vinothkumar and R. Henderson, "Structures of membrane proteins," *Q Rev Biophys*, vol. 43, pp. 65–158, Feb. 2010.

[21] D. Drew, L. Fröderberg, L. Baars, and J.-W. L. de Gier, "Assembly and overexpression of membrane proteins in Escherichia coli," *Biochim. Biophys. Acta*, vol. 1610, pp. 3–10, Feb. 2003.

[22] M. A. Lehrman, "A family of UDP-GlcNAc/MurNAc: polyisoprenol-P GlcNAc/MurNAc-1-P transferases.," *Glycobiology*, vol. 4, pp. 768–771, Dec. 1994.

[23] N. P. Price and F. A. Momany, "Modeling bacterial UDP-HexNAc: polyprenol-P HexNAc-1-P transferases," *Glycobiology*, vol. 15, pp. 29R–42R, Sept. 2005.

[24] M. S. Anderson, S. S. Eveland, and N. P. J. Price, "Conserved cytoplasmic motifs that distinguish sub-groups of the polyprenol phosphate:N-acetylhexosamine-1-phosphate transferase family," *FEMS Microbiol Lett*, vol. 191, pp. 169–175, Oct. 2000.

[25] A. Heifetz, R. W. Keenan, and A. D. Elbein, "Mechanism of action of tunicamycin on the UDP-GlcNAc:dolichyl-phosphate GlcNAc-1-phosphate transferase," *Biochemistry*, vol. 18, pp. 2186–2192, May 1979.

[26] J. A. Thanassi, S. L. Hartman-Neumann, T. J. Dougherty, B. A. Dougherty, and M. J. Pucci, "Identification of 113 conserved essential genes using a high-throughput gene disruption system in Streptococcus pneumoniae," *Nucleic Acids Res.*, vol. 30, pp. 3152–3162, July 2002.

[27] J. S. Anderson, M. Matsuhashi, M. A. Haskin, and J. L. Strominger, "LIPID-PHOSPHOACETYLMURAMYL-PENTAPEPTIDE AND LIPID-PHOSPHODISACCHARIDE-PENTAPEPTIDE: PRESUMED MEMBRANE TRANSPORT INTERMEDIATES IN CELL WALL SYNTHESIS," *Proc. Natl. Acad. Sci. U.S.A.*, vol. 53, pp. 881–889, Apr. 1965.

[28] W. G. Struve and F. C. Neuhaus, "EVIDENCE FOR AN INITIAL ACCEPTOR OF UDP-NAC-MURAMYL-PENTAPEPTIDE IN THE SYNTHESIS OF BACTERIAL MUCOPEPTIDE," *Biochem. Biophys. Res. Commun.*, vol. 18, pp. 6–12, Jan. 1965.

[29] T. D. H. Bugg, A. J. Lloyd, and D. I. Roper, "Phospho-MurNAc-pentapeptide translocase (MraY) as a target for antibacterial agents and antibacterial proteins," *Infect Disord Drug Targets*, vol. 6, pp. 85–106, June 2006.

[30] B. Al-Dabbagh, S. Olatunji, M. Crouvoisier, M. El Ghachi, D. Blanot, D. Mengin-Lecreulx, and A. Bouhss, "Catalytic mechanism of MraY and WecA, two paralogues of the polyprenyl-phosphate N-acetylhexosamine 1-phosphate transferase superfamily," *Biochimie*, vol. 127, pp. 249–257, Aug. 2016.

[31] A. Bouhss, M. Crouvoisier, D. Blanot, and D. Mengin-Lecreulx, "Purification and characterization of the bacterial MraY translocase catalyzing the first membrane step of peptidoglycan biosynthesis," *J. Biol. Chem.*, vol. 279, pp. 29974–29980, July 2004.

[32] A. E. Backmark, N. Olivier, A. Snijder, E. Gordon, N. Dekker, and A. D. Ferguson, "Fluorescent probe for high-throughput screening of membrane protein expression," *Protein Sci.*, vol. 22, pp. 1124–1132, Aug. 2013.

[33] Y. Ma, D. Münch, T. Schneider, H.-G. Sahl, A. Bouhss, U. Ghoshdastider, J. Wang, V. Dötsch, X. Wang, and F. Bernhard, "Preparative scale cell-free production and quality optimization of MraY homologues in different expression modes," *J. Biol. Chem.*, vol. 286, pp. 38844–38853, Nov. 2011.

[34] B. C. Chung, J. Zhao, R. A. Gillespie, D.-Y. Kwon, Z. Guan, J. Hong, P. Zhou, and S.-Y. Lee, "Crystal Structure of MraY, an Essential Membrane Enzyme for Bacterial Cell Wall Synthesis," vol. 341, p. 6, 2013.

[35] J. K. Hakulinen, J. Hering, G. Brändén, H. Chen, A. Snijder, M. Ek, and P. Johansson, "MraY–antibiotic complex reveals details of tunicamycin mode of action," *Nat Chem Biol*, vol. 13, pp. 265–267, Mar. 2017.

[36] B. C. Chung, E. H. Mashalidis, T. Tanino, M. Kim, A. Matsuda, J. Hong, S. Ichikawa, and S.-Y. Lee, "Structural insights into inhibition of lipid I production in bacterial cell wall synthesis," *Nature*, vol. 533, pp. 557–560, May 2016.

[37] E. H. Mashalidis, B. Kaeser, Y. Terasawa, A. Katsuyama, D.-Y. Kwon, K. Lee, J. Hong, S. Ichikawa, and S.-Y. Lee, "Chemical logic of MraY inhibition by antibacterial nucleoside natural products," *Nat Commun*, vol. 10, p. 2917, Dec. 2019.

[38] Y. Y. Dong, H. Wang, A. C. Pike, S. A. Cochrane, S. Hamedzadeh, F. J. Wyszyński, S. R. Bushell, S. F. Royer, D. A. Widdick, A. Sajid, H. I. Boshoff, Y. Park, R. Lucas, W.-M. Liu, S. S. Lee, T. Machida, L. Minall, S. Mehmood, K. Belaya, W.-W. Liu, A. Chu, L. Shrestha, S. M. Mukhopadhyay, C. Strain-Damerell, R. Chalk, N. A. Burgess-Brown, M. J. Bibb, C. E. Barry III, C. V. Robinson, D. Beeson, B. G. Davis, and E. P. Carpenter, "Structures of DPAGT1 Explain Glycosylation Disease Mechanisms and Advance TB Antibiotic Design," *Cell*, vol. 175, pp. 1045–1058.e16, Nov. 2018.

[39] J. Yoo, E. H. Mashalidis, A. C. Y. Kuk, K. Yamamoto, B. Kaeser, S. Ichikawa, and S.-Y. Lee, "GlcNAc-1-P-transferase–tunicamycin complex structure reveals basis for inhibition of N-glycosylation," *Nat Struct Mol Biol*, vol. 25, pp. 217–224, Mar. 2018.

[40] C. Dini, "MraY Inhibitors as Novel Antibacterial Agents," *Curr Top Med Chem*, vol. 5, no. 13, pp. 1221–1236, 2005.

[41] A. Takatsuki, K. Arima, and G. Tamura, "Tunicamycin, a new antibiotic. I. Isolation and characterization of tunicamycin," *J. Antibiot.*, vol. 24, pp. 215–223, Apr. 1971.

[42] A. J. Lloyd, P. E. Brandish, A. M. Gilbey, and T. D. H. Bugg, "Phospho-N-Acetyl-Muramyl-Pentapeptide Translocase from Escherichia coli: Catalytic Role of Conserved Aspartic Acid Residues," *J Bacteriol*, vol. 186, pp. 1747–1757, Mar. 2004.

[43] T. Stachyra, C. Dini, P. Ferrari, A. Bouhss, J. van Heijenoort, D. Mengin-Lecreulx, D. Blanot, J. Biton, and D. Le Beller, "Fluorescence detection-based functional assay for high-throughput screening for MraY," *Antimicrob. Agents Chemother.*, vol. 48, pp. 897–902, Mar. 2004.

[44] A. B. Shapiro, H. Jahić, N. Gao, L. Hajec, and O. Rivin, "A high-throughput, homogeneous, fluorescence resonance energy transfer-based assay for phospho-N-acetylmuramoyl-pentapeptide translocase (MraY)," *J Biomol Screen*, vol. 17, pp. 662–672, June 2012.

[45] S. Solapure, P. Raphael, C. Gayathri, S. Barde, B. .C, K. Das, and S. Desousa, "Development of a Microplate-Based Scintillation Proximity Assay for MraY Using a Modified Substrate," *Journal of biomolecular screening*, vol. 10, pp. 149–56, Apr. 2005.

[46] S. H. Lee, H. Wang, M. Labroli, S. Koseoglu, P. Zuck, T. Mayhood, C. Gill, P. Mann, X. Sher, S. Ha, S.-W. Yang, M. Mandal, C. Yang, L. Liang, Z. Tan, P. Tawa, Y. Hou, R. Kuvelkar, K. DeVito, X. Wen, J. Xiao, M. Batchlett, C. J. Balibar, J. Liu, J. Xiao, N. Murgolo, C. G. Garlisi, P. R. Sheth, A. Flattery, J. Su, C. Tan, and T. Roemer, "TarO-specific inhibitors of wall teichoic acid biosynthesis restore -lactam efficacy against methicillin-resistant staphylococci," *Sci Transl Med*, vol. 8, p. 329ra32, Mar. 2016.

[47] G. L. Wallis, F. W. Hemming, and J. F. Peberdy, "Investigation of the glycosyltransferase enzymes involved in the initial stages of the N-linked protein glycosylation pathway in Aspergillus niger," *Biochim. Biophys. Acta*, vol. 1426, pp. 91–98, Jan. 1999.

[48] N. P. Price, T. M. Hartman, J. Li, K. K. Velpula, T. A. Naumann, M. R. Guda, B. Yu, and K. M. Bischoff, "Modified tunicamycins with reduced eukaryotic toxicity that enhance the antibacterial activity of -lactams," *J Antibiot*, vol. 70, pp. 1070–1077, Nov. 2017.

[49] N. P. Price, M. A. Jackson, K. E. Vermillion, J. A. Blackburn, J. Li, and B. Yu, "Selective catalytic hydrogenation of the N-acyl and uridyl double bonds in the tunicamycin family of protein N-glycosylation inhibitors," *J Antibiot*, vol. 70, pp. 1122–1128, Dec. 2017.

[50] O. H. Hashim and W. Cushley, "Minor modifications to the structure of tunicamycin lead to loss of the biological activity of the antibiotic," *Biochimica et Biophysica Acta (BBA) - General Subjects*, vol. 923, pp. 362–370, Mar. 1987.

[51] B. C. Tsvetanova, D. J. Kiemle, and N. P. J. Price, "Biosynthesis of Tunicamycin and Metabolic Origin of the 11-Carbon Dialdose Sugar, Tunicamine," *J. Biol. Chem.*, vol. 277, pp. 35289–35296, Sept. 2002.

[52] K. Eckardt, "Tunicamycins, streptovirudins, and corynetoxins, a special subclass of nucleoside antibiotics," *J. Nat. Prod.*, vol. 46, pp. 544–550, Aug. 1983.

[53] N. P. Price, D. P. Labeda, T. A. Naumann, K. E. Vermillion, M. J. Bowman, M. A. Berhow, W. W. Metcalf, and K. M. Bischoff, "Quinovosamycins: new tunicamycin-type antibiotics in which the , -1,11-linked N-acetylglucosamine residue is replaced by N-acetylquinovosamine," *J Antibiot*, vol. 69, pp. 637–646, Aug. 2016.

[54] M. Batool, B. Ahmad, and S. Choi, "A Structure-Based Drug Discovery Paradigm," *International Journal of Molecular Sciences*, vol. 20, p. 2783, Jan. 2019.

[55] A. C. Anderson, "The Process of Structure-Based Drug Design," *Chemistry & Biology*, vol. 10, pp. 787–797, Sept. 2003.

[56] L. G. Ferreira, R. N. Dos Santos, G. Oliva, and A. D. Andricopulo, "Molecular docking and structure-based drug design strategies," *Molecules*, vol. 20, pp. 13384–13421, July 2015.

[57] X. Wang, K. Song, L. Li, and L. Chen, "Structure-Based Drug Design Strategies and Challenges," *Curr Top Med Chem*, vol. 18, no. 12, pp. 998–1006, 2018.

[58] R. M. Garavito and S. Ferguson-Miller, "Detergents as tools in membrane biochemistry," *J. Biol. Chem.*, vol. 276, pp. 32403–32406, Aug. 2001.

[59] E. S. Hemdan, Y. J. Zhao, E. Sulkowski, and J. Porath, "Surface topography of histidine residues: a facile probe by immobilized metal ion affinity chromatography.," *Proc Natl Acad Sci U S A*, vol. 86, pp. 1811–1815, Mar. 1989.

[60] N. Saraswathy and P. Ramalingam, "15 - Phosphoproteomics," in *Concepts and Techniques in Genomics and Proteomics* (N. Saraswathy and P. Ramalingam, eds.), Woodhead Publishing Series in Biomedicine, pp. 203–211, Woodhead Publishing, Jan. 2011.

[61] J. A. Bornhorst and J. J. Falke, "[16] Purification of Proteins Using Polyhistidine Affinity Tags," *Methods Enzymol*, vol. 326, pp. 245–254, 2000.

[62] P. Hong, S. Koza, and E. S. P. Bouvier, "A Review Size-Exclusion Chromatography for the Analysis of Protein Biotherapeutics and Their Aggregates," *Journal of Liquid Chromatography & Related Technologies*, vol. 35, pp. 2923–2950, Jan. 2012.

[63] K. Duquesne and J. N. Sturgis, "Membrane protein solubilization," *Methods Mol. Biol.*, vol. 601, pp. 205–217, 2010.

[64] J. M. Neugebauer, "[18] Detergents: An overview," in *Methods in Enzymology* (M. P. Deutscher, ed.), vol. 182 of *Guide to Protein Purification*, pp. 239–253, Academic Press, Jan. 1990.

[65] S. H. Lin and G. Guidotti, "Purification of membrane proteins.," *Methods Enzymol*, vol. 463, pp. 619–629, 2009.

[66] R. B. Sekar and A. Periasamy, "Fluorescence resonance energy transfer (FRET) microscopy imaging of live cell protein localizations," *J Cell Biol*, vol. 160, pp. 629–633, Mar. 2003.

[67] T. Förster, "Chapter II - Mechanisms of Energy Transfer," in *Comprehensive Biochemistry* (M. Florkin and E. H. Stotz, eds.), vol. 22 of *Bioenergetics*, pp. 61–80, Elsevier, Jan. 1967.

[68] E. B. V. Munster, G. J. Kremers, M. J. W. Adjobo-Hermans, and T. W. J. Gadella, "Fluorescence resonance energy transfer (FRET) measurement by gradual acceptor photobleaching," *Journal of Microscopy*, vol. 218, no. 3, pp. 253–262, 2005.

[69] R. M. Clegg, "Chapter 1 Förster resonance energy transfer—FRET what is it, why do it, and how it's done," in *Laboratory Techniques in Biochemistry and Molecular Biology*, vol. 33 of *Fret and Flim Techniques*, pp. 1–57, Elsevier, Jan. 2009.

[70] M. I. Recht, V. Nienaber, and F. E. Torres, "Chapter Three - Fragment-Based Screening for Enzyme Inhibitors Using Calorimetry," in *Methods in Enzymology* (A. L. Feig, ed.), vol. 567 of *Calorimetry*, pp. 47–69, Academic Press, Jan. 2016.

[71] V. K. Srivastava and R. Yadav, "Chapter 9 - Isothermal titration calorimetry," in *Data Processing Handbook for Complex Biological Data Sources* (G. Misra, ed.), pp. 125–137, Academic Press, Jan. 2019.

[72] L. Mazzei, S. Ciurli, and B. Zambelli, "Chapter Nine - Isothermal Titration Calorimetry to Characterize Enzymatic Reactions," in *Methods in Enzymology* (A. L. Feig, ed.), vol. 567 of *Calorimetry*, pp. 215–236, Academic Press, Jan. 2016.

[73] C. Dalvit, G. Fogliatto, A. Stewart, M. Veronesi, and B. Stockman, "WaterLOGSY as a method for primary NMR screening: practical aspects and range of applicability," *J. Biomol. NMR*, vol. 21, pp. 349–359, Dec. 2001.

[74] A. Kumar and R. Christy Rani Grace, "Nuclear Overhauser Effect," in *Encyclopedia of Spectroscopy and Spectrometry* (J. C. Lindon, ed.), pp. 1643–1653, Oxford: Elsevier, Jan. 1999.

[75] R. Huang, A. Bonnichon, T. D. W. Claridge, and I. K. H. Leung, "Protein-ligand binding affinity determination by the waterLOGSY method: An optimised approach considering ligand rebinding," *Sci Rep*, vol. 7, Mar. 2017.

[76] G. Senisterra, I. Chau, and M. Vedadi, "Thermal denaturation assays in chemical biology," *Assay Drug Dev Technol*, vol. 10, pp. 128–136, Apr. 2012.

[77] H. L. Silvestre, T. L. Blundell, C. Abell, and A. Ciulli, "Integrated biophysical approach to fragment screening and validation for fragment-based lead discovery," *Proc. Natl. Acad. Sci. U.S.A.*, vol. 110, pp. 12984–12989, Aug. 2013.

[78] D. Toledo Warshaviak, G. Golan, K. W. Borrelli, K. Zhu, and O. Kalid, "Structure-based virtual screening approach for discovery of covalently bound ligands," *J Chem Inf Model*, vol. 54, pp. 1941–1950, July 2014.

[79] R. A. Friesner, J. L. Banks, R. B. Murphy, T. A. Halgren, J. J. Klicic, D. T. Mainz, M. P. Repasky, E. H. Knoll, M. Shelley, J. K. Perry, D. E. Shaw, P. Francis, and P. S. Shenkin, "Glide: a new approach for rapid, accurate docking and scoring. 1. Method and assessment of docking accuracy," *J. Med. Chem.*, vol. 47, pp. 1739–1749, Mar. 2004.

[80] R. A. Friesner, R. B. Murphy, M. P. Repasky, L. L. Frye, J. R. Greenwood, T. A. Halgren, P. C. Sanschagrin, and D. T. Mainz, "Extra precision glide: docking and scoring incorporating a model of hydrophobic enclosure for protein-ligand complexes," *J. Med. Chem.*, vol. 49, pp. 6177–6196, Oct. 2006.

[81] N. E. Chayen and E. Saridakis, "Protein crystallization: from purified protein to diffraction-quality crystal," *Nat Methods*, vol. 5, pp. 147–153, Feb. 2008.

[82] A. McPherson and J. A. Gavira, "Introduction to protein crystallization," *Acta Crystallogr F Struct Biol Commun*, vol. 70, pp. 2–20, Jan. 2014.

[83] P. G. Vekilov, "Phase diagrams and kinetics of phase transitions in protein solutions," *J Phys Condens Matter*, vol. 24, p. 193101, May 2012.

[84] J. Manuel García-Ruiz, "Nucleation of protein crystals," *J. Struct. Biol.*, vol. 142, pp. 22–31, Apr. 2003.

[85] E. P. Carpenter, K. Beis, A. D. Cameron, and S. Iwata, "Overcoming the challenges of membrane protein crystallography," *Current Opinion in Structural Biology*, vol. 18, pp. 581–586, Oct. 2008.

[86] S. Iwata, *Methods and Results in Crystallization of Membrane Proteins*. Internat'l University Line, 2003. Google-Books-ID: sMS_3SbWUjsC.

[87] S. Newstead, S. Ferrandon, and S. Iwata, "Rationalizing alpha-helical membrane protein crystallization," *Protein Sci.*, vol. 17, pp. 466–472, Mar. 2008.

[88] E. M. Landau and J. P. Rosenbusch, "Lipidic cubic phases: A novel concept for the crystallization of membrane proteins," *PNAS*, vol. 93, pp. 14532–14535, Dec. 1996.

[89] J. Zha and D. Li, "Lipid Cubic Phase for Membrane Protein X-ray Crystallography," in *Membrane Biophysics: New Insights and Methods* (H. Wang and G. Li, eds.), pp. 175–220, Singapore: Springer, 2018.

[90] J. Hering, E. Dunevall, M. Ek, and G. Brändén, "Structural basis for selective inhibition of antibacterial target MraY, a membrane-bound enzyme involved in peptidoglycan synthesis," *Drug Discovery Today*, vol. 23, pp. 1426–1435, July 2018.

[91] R. Bretthauer, "Structure, Expression, and Regulation of UDP-GlcNAc: Dolichol Phosphate GlcNAc-1-Phosphate Transferase (DPAGT1)," *CDT*, vol. 10, pp. 477–482, June 2009.

[92] B. Al-Dabbagh, X. Henry, M. El Ghachi, G. Auger, D. Blanot, C. Parquet, D. Mengin-Lecreulx, and A. Bouhss, "Active site mapping of MraY, a member of the polyprenyl-phosphate N-acetylhexosamine 1-phosphate transferase superfamily, catalyzing the first membrane step of peptidoglycan biosynthesis," *Biochemistry*, vol. 47, pp. 8919–8928, Aug. 2008.

[93] G. G. Privé, "Detergents for the stabilization and crystallization of membrane proteins," *Methods*, vol. 41, pp. 388–397, Apr. 2007.

[94] M. Castaldo, L. Barlind, F. Mauritzson, P. T. Wan, and H. J. Snijder, "A fast and easy strategy for protein purification using "teabags"," *Sci Rep*, vol. 6, June 2016.

[95] R. M. Bill, P. J. F. Henderson, S. Iwata, E. R. S. Kunji, H. Michel, R. Neutze, S. Newstead, B. Poolman, C. G. Tate, and H. Vogel, "Overcoming barriers to membrane protein structure determination," *Nat. Biotechnol.*, vol. 29, pp. 335–340, Apr. 2011.

[96] C. Montigny, T. Dieudonné, S. Orlowski, J. L. Vázquez-Ibar, C. Gauron, D. Georgin, S. Lund, M. le Maire, J. V. Møller, P. Champeil, and G. Lenoir, "Slow Phospholipid Exchange between a Detergent-Solubilized Membrane Protein and Lipid-Detergent Mixed Micelles: Brominated Phospholipids as Tools to Follow Its Kinetics," *PLoS ONE*, vol. 12, no. 1, p. e0170481, 2017.

[97] P. A. Cockrum and J. A. Edgar, "High-performance liquid chromatograpic comparison of the tunicaminyluracil-based antibiotics corynetoxin, tunicamycin, streptovirudin and MM 19290," *Journal of Chromatography A*, vol. 268, pp. 245–254, Jan. 1983.

[98] K. Yamamoto, T. Sato, Y. Hikiji, A. Katsuyama, T. Matsumaru, F. Yakushiji, S.-I. Yokota, and S. Ichikawa, "Synthesis and biological evaluation of a MraY selective analogue of tunicamycins," *Nucleosides, Nucleotides and Nucleic Acids*, pp. 1–16, Sept. 2019.

[99] T. Mohammadi, A. Karczmarek, M. Crouvoisier, A. Bouhss, D. Mengin-Lecreulx, and T. D. Blaauwen, "The essential peptidoglycan glycosyltransferase MurG forms a complex with proteins involved in lateral envelope growth as well as with proteins involved in cell division in Escherichia coli," *Molecular Microbiology*, vol. 65, no. 4, pp. 1106–1121, 2007.

[100] S. Hirano, S. Ichikawa, and A. Matsuda, "Structure–activity relationship of truncated analogs of caprazamycins as potential anti-tuberculosis agents," *Bioorganic & Medicinal Chemistry*, vol. 16, pp. 5123–5133, May 2008.

[101] S. Hirano, S. Ichikawa, and A. Matsuda, "Design and synthesis of diketopiperazine and acyclic analogs related to the caprazamycins and liposidomycins as potential antibacterial agents," *Bioorganic & Medicinal Chemistry*, vol. 16, pp. 428–436, Jan. 2008.

[102] E. Henrich, Y. Ma, I. Engels, D. Münch, C. Otten, T. Schneider, B. Henrichfreise, H.-G. Sahl, V. Dötsch, and F. Bernhard, "Lipid Requirements for the Enzymatic Activity of MraY Translocases and *in Vitro* Reconstitution of the Lipid II Synthesis Pathway," *J. Biol. Chem.*, vol. 291, pp. 2535–2546, Jan. 2016.